2 The Tuscany Province

Abstract

The Tuscany Magmatic Province consists of various intrusive and extrusive bodies ranging in composition from mafic to felsic and from calcalkaline to ultrapotassic lamproitic. Rock age ranges from about 8 to 0.3 Ma, and decreases eastward from the Tuscan Archipelago to the Southern Tuscany mainland. An isolated sill from Sisco (Alpine Corsica, 14.5 Ma) is also included in the Tuscany Province. Silicic magmas make up several granitoid bodies and minor lavas. They are polygenetic and have been formed by crustal melting, mixing between crustal anatectic and minor amounts of mafic melts, and fractional crystallisation or AFC of intermediate-mafic parents. Except for the Capraia Island stratovolcano, mafic-intermediate rocks mostly occur as small subvolcanic and extrusive bodies, and as mafic enclaves in the silicic rocks. Mafic magmas originated within the upper mantle but have striking crustal-like trace element and radiogenic isotope signatures, resembling closely some upper crustal rocks such as metapelites. The coexistence of both crustal and mantle signatures in these magmas reveals an origin from anomalous sources, consisting of a mélange of mantle and crustal rocks. Such a particular type of source in Tuscany probably formed during the Late Cretaceous to Eocene subduction of the European plate beneath the African margin. Partial melting of subduction mélange took place much later, during the Miocene to present opening of the northern Tyrrhenian Sea behind the west dipping and eastward retreating Adriatic subducting slab. Age polarity of Tuscany magmatism reflects the timing of backarc extension that migrated from west to the east.

Keywords

Tuscany magmatism · Crustal anatexis · Granitoids · Calcalkaline magmas · Lamproites · Adakite · Mantle contamination · Subduction mélange · Northern Apennines · Geodynamics

A. Peccerillo, *Cenozoic Volcanism in the Tyrrhenian Sea Region*,
Advances in Volcanology, DOI 10.1007/978-3-319-42491-0_2

2.1 Introduction

The Tuscany Magmatic Province (Fig. 2.1) consists of several mafic to silicic intrusive and extrusive centres scattered through southern Tuscany, the Tuscan Archipelago and northern Latium. An older mafic ultrapotassic sill from Sisco (northeastern Alpine Corsica) is here included into the Tuscany Province, because of its lamproitic composition similar to some Tuscany occurrences.

The Tuscany igneous rocks form stocks, dikes, necks, lava flows and domes, and the large volcanoes of the Island of Capraia, Monte Amiata, and Monti Cimini. Pyroclastic rocks occur as ignimbritic deposits at Monti Cimini and Cerite area (e.g. Poli et al. 2003; Cimarelli and De Rita 2006a, b; LaBerge et al. 2006), but are scarce or absent in other Tuscany centres. Ages range from about 8.5 Ma for some rocks in the Elba island to about 0.3 Ma for Monte Amiata and show a tendency to decrease from west to east (Fig. 2.1). The Sisco rock is about 14.5 Ma old (Civetta et al. 1978).

Although volumetrically subordinate with respect to other volcanic provinces in Italy, the Tuscany magmatism exhibits an extreme compositional complexity, which calls for the interplay of several mechanisms of magma genesis and evolution, and various types of mantle and crustal sources. An overview of magmatic centres is given in Table 2.1. Representative whole rock analyses are given in Table 2.2.

2.2 Regional Geology

The geology of Tuscany consists of stacked tectonic thrust units, mostly verging eastwards, overlain by Mio-Pleistocene post-orogenic neo-

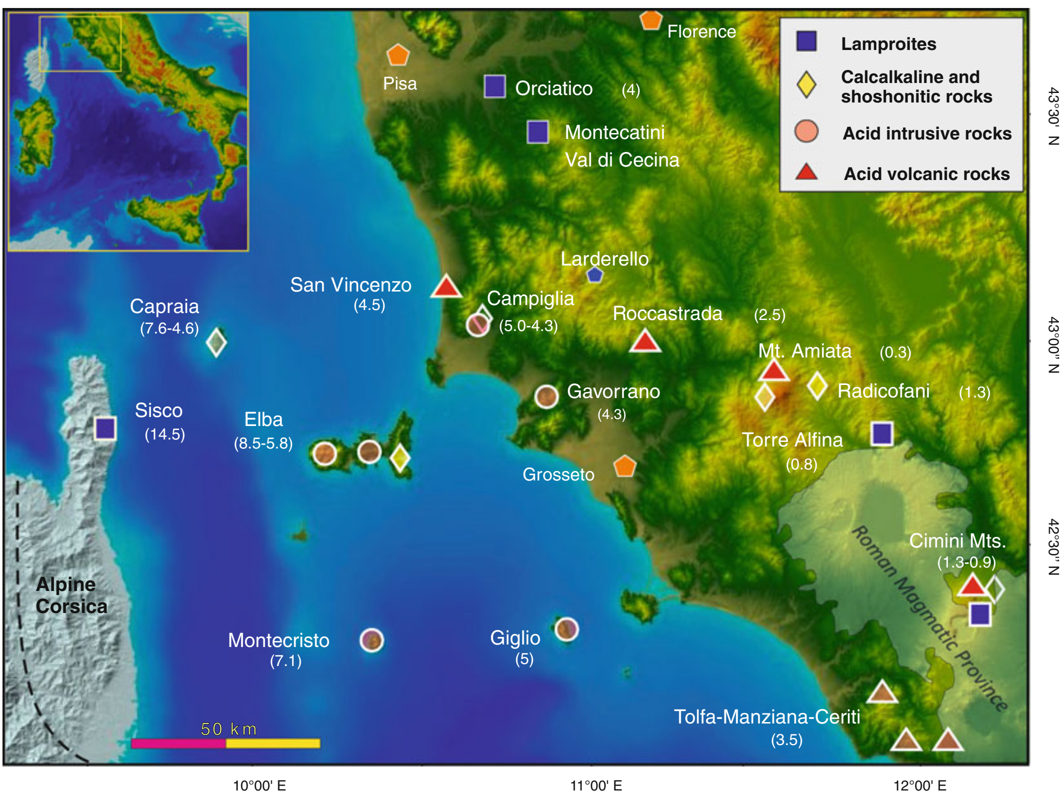

Fig. 2.1 Location of intrusive and extrusive centres of the Tuscany Magmatic Province. Numbers in parentheses indicate ages (in Ma). Relief shaded map from Tarquini et al. (2012)

Table 2.1 Petrological characteristics and ages (in Ma) of magmatic centres in the Tuscany Province

Magmatic centres	Age (Ma)	Occurrence	Petrology-geochemistry
Silicic volcanic centres			
San Vincenzo	4.5	– Lava flows and domes	– Calcalkaline peraluminous rhyolites containing latite enclaves. Variable Sr isotope ratios ($^{87}Sr/^{86}Sr \sim 0.713–0.725$) resulting from mixing of crustal anatectic rhyolites and mafic magmas
Tolfa-Manziana-Cerite	3.5	– Dome complex and pyroclastic deposits strongly affected by secondary alteration	– Trachydacites to high-silica rhyolites, containing abundant mafic enclaves. Formed by crustal melting plus fractional crystallisation and mixing with mafic magmas
Roccastrada	2.5	– Lava flows and dome	– Calcalkaline peraluminous rhyolites with $^{87}Sr/^{86}Sr \sim 0.7182$ to 0.7198, originated by crustal melting
Monte Amiata	0.3	– Central cone made of prevailing silicic lava flows and domes, with a few late mafic lavas	– Dominant trachydacites with minor olivine-latites and shoshonites. Origin by mixing of crustal anatectic melts and mafic Roman-type potassic alkaline magmas
Silicic plutonic centres			
Island of Elba	8.5–5.8	– Monzogranite stock with aplites and pegmatites (Mt. Capanne) and various laccoliths, dikes and sills. Late mafic dikes	– Dominant acid peraluminous monzogranites and granodiorites containing microgranular mafic enclaves, formed by crustal anatexis plus interaction with calcalkaline mantle-derived magmas, and fractional crystallisation. Late intrusion of mantle-derived shoshonitic dikes
Vercelli Seamount	7.2	– Seamount with summit at a depth of about 58 m bsl	– Syenogranitic composition, based on a single sample
Island of Montecristo	7.1	– Monzogranite stock cut by aplite and pegmatite veins and porphyritic dikes	– Peraluminous monzogranite stock cut by andesitic dikes. Origin by mixing of crustal anatectic and mafic calcalkaline magma, plus late intrusion of shoshonites
Island of Giglio	5	– Multiple intrusions of monzogranite, leucocratic monzogranite, and aplite-pegmatite	– Calcalkaline peraluminous rocks with variable $^{87}Sr/^{86}Sr$ ($\sim 0.7163–0.7203$) increasing from monzogranites to leucogranites. Similar origin to other Tuscany granitoids
Campiglia	5	– Stock mostly hidden beneath surface. Younger felsic and mafic porphyritic dikes in the same area	– Intensely altered monzogranite to alkali-feldspar granite depleted in Fe by secondary processes
Gavorrano	4.3	– Intrusive body forming a 3 km NNW elongated outcrop	– Monzogranite to tourmaline-rich alkali feldspar granite. Same origin as other Tuscany granitoids
Hidden intrusions	5 - 0?	– Various bodies near Campiglia and Gavorrano, and in the Larderello area, the latter being still partially molten	– Granitoid rocks (monzogranites, syenogranites, granodiorite etc.) with $^{87}Sr/^{86}Sr \sim 0.7145–0.7222$. Formed by crustal anatexis plus probable mixing with mafic melts
Mafic volcanic and hypabyssal centres			
Sisco	14.5	– Thin sill cutting through high-P Alpine metamorphic units	– Peralkaline high-silica lamproite originated in mantle sources contaminated by siliceous rocks

(continued)

Table 2.1 (continued)

Magmatic centres	Age (Ma)	Occurrence	Petrology-geochemistry
Island of Capraia	7.6-4.6	– Remnants of a large stratovolcano formed mainly of intermediate lavas. Final mafic lavas and scoriae	– Dominant high-K calcalkaline andesites and dacites, and final shoshonitic basalts, showing the least radiogenic Sr isotope composition in Tuscany ($^{87}Sr/^{86}Sr$ = 0.7073-0.7102). Occurrence of Sr-Ba- LREE rich adakite-type intermediate magmas. Formed by melting of sources less contaminated than at other Tuscany mafic centres
Campiglia	4.3	– N-S trending strongly altered mafic dikes	– Ultrapotassic rocks showing trace element and Sr isotopic compositions similar to Capraia calcalkaline rocks. Ultrapotassic composition probably related to secondary processes
Montecatini Val di Cecina	4.1	– Phologopite-rich plug permeated by abundant leucocratic veinlets	– High-silica lamproite with higher Sr isotope ratios than Sisco ($^{87}Sr/^{86}Sr$ = 0.7169). Formed by melting of anomalous lithospheric mantle, contaminated by crustal siliceous rocks. Veinlets generated by unmixing from the partially crystallised host intrusion
Orciatico	4.1	– Mafic hypabyssal body	– High-silica lamproite with composition and origin similar to Montecatini Val di Cecina
Monti Cimini	1.3-0.9	– Early felsic lava domes and flows, and ignimbrites followed by intermediate to mafic lavas	– Shoshonitic to ultrapotassic trachytes, trachydacites, latites and shoshonites showing variable $^{87}Sr/^{86}Sr$ (~0.7122–0.7157) in the mafic rocks. Melting of heterogeneous mantle sources and mixing with crustal anatectic melts
Radicofani	1.3	– Mafic neck and remnants of lava flows	– Basaltic andesite to shoshonite formed by mixing between high-silica lamproite and calcalkaline basalt magmas
Torre Alfina	0.8	– Mafic necks and lava flows containing crustal xenoliths and some high-P ultramafic nodules	– High-silica lamproite with composition and origin similar to Montecatini and Orciatico

autochthonous sediments (e.g. Abbate et al. 1970; Barchi et al. 2001; Carmignani et al. 2001). The main tectono-stratigraphic units include:

1. Paleozoic metamorphic rocks (quartz-metaconglomerates, quartzites, phyllites, metavolcanics and micaschists) that have been affected by Alpine metamorphism and are superimposed over a gneiss complex;
2. The Tuscan units consisting of Late Triassic to early Miocene sedimentary rocks (conglomerates, evaporites, limestones, marls and arenaceous flysch) overlying the metamorphic basement, and affected by Alpine metamorphism in some places (e.g. Alpi Apuane);
3. The Ligurian complex tectonically superimposed on the Tuscan units, consisting of middle to late Jurassic ophiolites and radiolarites plus Cretaceous to Eocene pelagic limestones and flysch sequences;
4. Oligo-Miocene clastic marine sediments resting unconformably over the Liguride sequences;
5. Neo-autochthonous Miocene to Pleistocene sediments (evaporites, lignite, fresh water limestones, conglomerates, clays, sands, etc.) infilling tectonic depressions.

These rock units were formed during a complex series of tectonic events, which include

Table 2.2 Compositions of representative igneous rocks from Tuscany

Magmatic centre	Roccastrada	San Vincenzo	Tolfa	Manziana	Mt. Amiata	Mt. Amiata	Mt. Cimini	Mt. Cimini
Rock type	Rhyolite	Rhyolite	Latite	Rhyolite	Trachydacite	Mafic enclave	Trachydacite	Latite
Data source	4,1,2	4,1,2	5	5	13	13	20	20
SiO_2 wt%	72.48	68.76	64.61	71.66	64.90	53.76	64.16	56.94
TiO_2	0.24	0.38	0.66	0.39	0.57	0.72	0.69	1.10
Al_2O_3	13.56	14.94	16.45	14.50	15.90	17.16	16.60	15.39
FeO_{total}	1.91	2.33	3.57	2.19	3.88	6.02	4.41	4.80
MnO	0.03	0.03	0.04	0.03	0.06	0.10	0.08	0.10
MgO	0.36	0.91	1.40	0.31	1.74	4.64	2.18	7.65
CaO	1.02	1.96	3.18	1.51	2.97	6.85	3.16	5.50
Na_2O	2.61	2.86	2.47	3.28	2.08	1.64	2.31	1.33
K_2O	4.86	4.63	5.23	4.99	5.2	5.27	5.18	5.77
P_2O_5	0.14	0.20	0.12	0.03	0.2	0.28	0.21	0.27
LOI	1.56	1.93	1.98	0.81	1.92	2.76	0.83	1.01
Sc ppm	5	6	–	–	(12)	(37)	10.7	(21)
V	12	36	–	–	59	141	57	103
Cr	10	28	–	–	31	121	32	389
Co	2	5	–	–	–	–	9	–
Ni	19	21	–	–	14	40	20	154
Rb	395	310	305	385	369	295	290	382
Sr	68	223	264	91	282	663	416	409
Y	33	24	28	35	27	32	31	23
Zr	113	149	275	214	265	288	262	429
Nb	14	13	19	10	17	14	19	24
Cs	(13.8)	–	–	–	26.01	18.09	(33)	(27)
Ba	172	400	567	231	343	781	764	756
La	30	43	51	71	71	74	95	93
Ce	68	91	97	133	142	146	155	193
Nd	29	43	36	50	57	68	55	85
Sm	6.8	8.9	6.7	9.4	10.28	12.19	12.8	15.9
Eu	0.6	1.3	1.2	0.82	1.16	2.18	1.69	2.32
Tb	1.1	1.0	–	–	1.02	1.15	0.99	1.10
Yb	3.1	1.8	2.4	3.4	2.7	2.61	2.40	1.96
Lu	0.3	0.2	0.5	0.63	0.41	0.39	0.50	0.34
Hf	3.8	4.1	–	–	7.49	7.21	7.0	10.9
Ta	(1.83)	(1.9)	–	–	1.7	1.12	1.8	1.9
Pb	45	50	56	75	57	52	69	49
Th	24	20	30	53	43	36	45	58
U	17	11	8.7	10	11.2	8.36	6.9	8.5
$^{87}Sr/^{86}Sr$	0.71799	0.71558	0.71383	0.71308	0.712574	0.71139	0.713902	0.715648
$^{143}Nd/^{144}Nd$	(0.51221)	(0.51225)	–	–	0.512096	0.51209	0.512139	0.512063
$^{206}Pb/^{204}Pb$	(18.68)	(18.71)	18.74	18.723	18.721	18.731	18.708	18.723

(continued)

Table 2.2 (continued)

Magmatic centre	Roccastrada	San Vincenzo	Tolfa	Manziana	Mt. Amiata	Mt. Amiata	Mt. Cimini	Mt. Cimini
Rock type	Rhyolite	Rhyolite	Latite	Rhyolite	Trachydacite	Mafic enclave	Trachydacite	Latite
$^{207}Pb/^{204}Pb$	(15.65)	(15.66)	15.70	15.663	15.681	15.678	15.671	15.689
$^{208}Pb/^{204}Pb$	(38.91)	(38.88)	38.79	38.859	39.003	39.002	38.959	39.023

Magmatic centre	Capraia	Capraia	Sisco	Montecatini Val di Cecina	Orciatico	Torre Alfina	Radicofani
Rock type	Shoshonitic basalt	Andesite	Lamproite	Lamproite	Lamproite	Lamproite	Shoshonite
Data source	14	14	12,15,17	12,15, 17	12,15, 17	18,17	18,10
SiO_2 wt%	50.65	61.90	58.50	56.86	57.79	55.50	54.30
TiO_2	1.65	0.69	2.27	1.37	1.51	1.36	0.91
Al_2O_3	15.50	15.30	10.84	12.61	11.79	13.40	17.21
FeO_{total}	9.18	4.85	3.15	5.76	5.13	5.78	6.07
MnO	0.13	0.07	0.06	0.1	0.08	0.10	0.11
MgO	6.41	3.48	6.63	7.15	8.23	9.36	7.77
CaO	7.92	5.48	3.12	3.47	3.46	4.70	7.59
Na_2O	2.83	3.14	1.02	1.2	1.31	1.18	2.02
K_2O	2.42	3.33	10.73	7.91	8.06	7.46	2.89
P_2O_5	0.48	0.18	0.67	0.92	0.85	0.54	0.25
LOI	1.13	1.36	2.09	2.43	1.55	0.58	0.84
Sc ppm	23	–	11	20.2	18.5	17	(23)
V	166	128	84	137	116	118	173
Cr	400	177	340	380	500	641	417
Co	30	11.9	19	27	28.1	36	29.4
Ni	69	29	230	140	280	349	124
Rb	115	116	318	768	612	453	168
Sr	399	733	640	408	577	726	339
Y	20	19.3	19	28	23.8	33	22.6
Zr	221	185	1040	491	749	674	216
Nb	15	11.9	55	30.1	39	31	11.7
Cs	4	9.2	2	14	25.2	30	9.46
Ba	540	711	1450	1370	1400	1293	579
La	29	58.5	183	79.8	148	98	41.4
Ce	68	109	367	206	352	294	92.6
Nd	51.9	43.6	146	133	193	127	43.6
Sm	9.6	8.01	19.1	23.5	26.9	20.7	7.7
Eu	2.09	1.76	3.5	4.02	4.32	3.51	1.75
Tb	1	0.77	1.09	1.31	1.27	1.2	0.81
Yb	2.3	1.84	1.59	2.19	1.85	2.38	1.97
Lu	0.35	0.28	0.21	0.3	0.25	0.39	0.32
Hf	5.6	5.4	32.1	13.4	21.4	15.5	5.48
Ta	1.2	0.9	3.96	2.17	2.93	2.3	0.95
Pb	12	61	12	19	30	57	29
Th	24	23.1	37.9	112	119	61	24.7
U	3.8	6.43	4.61	18.2	14.9	14.2	4.62

(continued)

Table 2.2 (continued)

Magmatic centre	Capraia	Capraia	Sisco	Montecatini Val di Cecina	Orciatico	Torre Alfina	Radicofani
Rock type	Shoshonitic basalt	Andesite	Lamproite	Lamproite	Lamproite	Lamproite	Shoshonite
$^{87}Sr/^{86}Sr$	0.708135	0.708719	0.712264	0.71672	0.71579	0.71579	0.71333
$^{143}Nd/^{144}Nd$	0.512254	0.512346	0.512149	0.512086	0.512094	0.51212	0.51218
$^{206}Pb/^{204}Pb$	18.652	18.735	18.808	18.624	18.697	18.677	18.711
$^{207}Pb/^{204}Pb$	15.663	15.702	15.696	15.638	15.698	15.678	15.665
$^{208}Pb/^{204}Pb$	38.963	39.086	39.190	38.947	39.062	38.918	39.049
$^{176}Hf/^{177}Hf$	–	–	0.282504	0.282435	0.282404	0.282398	0.282554

Magmatic centre	Elba			Montecristo	Giglio		Larderello	Vercelli Seamount
Rock type	Monzo-granite	Syeno-granite	Andesitic dike	Monzo-granite	Monzogranite	Leucogranite	Granite Monteverdi Drilling	Syenogranite
Data source	9,16,1	19	21	6, 8	6, 7	6, 7	11	3
SiO_2 wt%	67.49	70.79	62.77	70.55	67.63	73.54	70.06	72.60
TiO_2	0.52	0.32	0.66	0.36	0.66	0.21	0.37	0.23
Al_2O_3	15.69	15.74	15.25	14.94	15.56	14.07	15.53	14.23
FeO	2.68	2.18	4.51	2.10	3.73	1.47	2.39	1.59
MnO	0.05	0.04	0.07	0.04	0.08	0.05	<0.02	0.04
MgO_{total}	1.57	0.74	3.79	0.66	1.24	0.38	0.76	0.50
CaO	2.7	1.65	2.42	1.76	2.13	0.82	1.90	1.05
Na_2O	3.53	3.16	3.03	3.71	2.81	2.38	2.94	3.91
K_2O	4.13	4.45	3.08	4.77	4.79	6.04	4.66	4.51
P_2O_5	0.2	0.17	0.17	0.22	0.17	0.14	0.16	0.26
LOI	1.14	1.21	3.32	0.64	1.11	0.89	0.80	0.90
Sc ppm	8.3	5.0	14	6.1	10.7	4	–	–
V	36	24.0	91	–	–	–	34.3	17
Cr	30.6	15.0	190	28	44	4	25.7	12
Co	7.2	4.0	14	5	8.5	4	5.3	–
Ni	13.4	10.0	20	–	–	–	13	–
Rb	275	294	65	357	337	372	238	440
Sr	229	126	316	122	131	65	305	302
Y	20	12.1	18	22	30	21	13.2	19
Zr	–	–	143	116	223	92	148	87
Nb	13.1	11.8	10.5	6	12	11	8.8	–
Cs	41.5	34	2.6	–	–	–	13.7	–
Ba	402	257	425	293	318	74	601	112
La	33.7	28.9	29.2	30	44	16	28	28
Ce	68.9	60.0	56	61	96	39	58.8	36
Nd	29.7	24.8	25.7	27	41	18.6	24	–
Sm	5.96	5.0	5.19	5.8	8.8	4.6	4.7	–
Eu	0.92	0.68	1.18	0.7	1.1	0.48	0.87	–
Tb	0.63	0.48	0.63	0.6	1.0	0.55	0.44	–
Yb	1.35	0.73	1.75	1.7	2.7	2.8	1.17	–

(continued)

Table 2.2 (continued)

Magmatic centre	Elba			Montecristo	Giglio		Larderello	Vercelli Seamount
Rock type	Monzo-granite	Syeno-granite	Andesitic dike	Monzo-granite	Monzogranite	Leucogranite	Granite Monteverdi Drilling	Syenogranite
Lu	0.18	0.09	0.26	0.30	0.45	0.46	0.17	–
Hf	(3.3)	0.33	3.8	–	5.5	2.8	4.35	–
Ta	1.79	2.30	1.03	–	2.5	1.1	1.07	–
Pb	43.7	33	18	–	–	–	44.7	–
Th	19.5	11.6	12.6	30	21	10	21.2	11
U	14.4	7.4	6.17	–	–	–	10.3	7
$^{87}Sr/^{86}Sr$	0.71461	0.722800	0.708129	(0.71466)	(0.7173)	(0.7195)	0.719075	0.71140
$^{143}Nd/^{144}Nd$	0.512182	0.512117	0.512209	–	(0.5122)	(0.5121)	0.512086	–
$^{206}Pb/^{204}Pb$	(18.68)	–	–	–	–	–	–	–
$^{207}Pb/^{204}Pb$	(15.67)	–	–	–	–	–	–	–
$^{208}Pb/^{204}Pb$	(38.87)	–	–	–	–	–	–	–

Source of data: (1) Vollmer (1977); (2) Hawkesworth and Vollmer (1979); (3) Barbieri et al. (1986); (4) Giraud et al. (1986); (5) Pinarelli (1991); (6) Poli (1992); (7) Westerman et al. (1993); (8) Innocenti et al. (1997); (9) Dini et al. (2002); (10) Gasperini et al. (2002); (11) Dini et al. (2005); (12) Conticelli et al. (2007); (13) Cadoux and Pinti (2009); (14) Conticelli et al. (2009a, b); (15) Conticelli et al. (2010); (16) Farina et al. (2010); (17) Prelevic et al. (2010); (18) Conticelli et al. (2011); (19) Farina et al. (2012); (20) Conticelli et al. (2013); (21) Pandeli et al. (2014)

rifting, oceanic convergence, continental collision and post-orogenic extension. Early rifting occurred during Triassic-Jurassic times; continental to littoral clastic sediments, evaporitic deposits and carbonate rocks, as well as ophiolitic sequences of the Liguride units were formed during this phase (e.g. Principi and Treves 1984; Balestrieri et al. 2011). Compression started during Cretaceous in the Liguride units and continued during the Lower Oligocene when the Tuscan units were tectonically emplaced over the Umbria sequences on the east. Successively, the compressive front shifted eastward involving progressively more external sectors of the Adriatic foreland (Brunet et al. 2000; Barchi 2010 with references). Contemporaneously, extension and magmatism affected the backarc area, migrating from west to east behind the shifting compressive front of Northern Apennines (e.g. Civetta et al. 1978; Peccerillo et al. 1987; Serri et al. 1993; Pauselli et al. 2006; Pandeli et al. 2010). According to Boccaletti et al. (1997), extensional tectonic regime west of the compression front was interrupted by Messinian, Late Pliocene and Middle Pleistocene compressive tectonic phases, which would be responsible for interruption of magmatic activity in these periods.

Syn-tectonic terrigenous turbidite and pelagic sedimentation, thrusting and HP–LT to Barrovian metamorphism took place during the compressional tectonic phases. Synorogenic metamorphic rocks are exposed at various localities of the mainland Tuscany, Tuscan archipelago and northeastern Corsica (Alpine Corsica). Peak pressures of 1.3–1.6 GPa at temperatures of about 300–420 °C were found for the *Schistes Lustrés* in the Corsica and Gorgona islands, whereas lower pressures of 0.6–0.85 GPa have been determined for the same units in the Giglio area (Franceschelli et al. 2004 with references), and for Cretaceous metabasites at Elba (P ~ 1 GPa, T = 300–350 °C; Bianco et al. 2015). A younger metamorphic phase took place in the Miocene during extension and rapid exhumation (Balestrieri et al. 2011).

Moho is about 20 km deep and asthenosphere occurs at 40–50 km beneath the Tyrrhenian border of southern Tuscany; crustal thickness increases eastward reaching a maximum of about 40 km beneath the axial zone of the Apennines (e.g. Gianelli et al. 1997; Piromallo and Morelli

2003; Mele and Sandvol 2003; Mele et al. 2006; Di Stefano et al. 2011; Carannante et al. 2013; Buttinelli et al. 2014). A vertical zone with high seismic-wave velocity has been detected beneath the Northern Apennines (e.g. Panza and Mueller 1979; Benoit et al. 2011). This has been interpreted as a remnant lithospheric slab from the Adriatic plate (east of the Apennine chain), which is passively sinking into the upper mantle. According to recent studies, the slab extends to about 300 km depth, with its southern edge at about 43°N, with no deep continuity with any slab segment to the south (Benoit et al. 2011). An additional important geophysical feature is denoted by the occurrence of a high-Vp anomaly at about 40–50 km depth beneath the westernmost sector of the Tuscany Magmatic Province. This may represent the remnants of the European lithosphere subducted during Alpine orogenic phase (Finetti et al. 2001; Pauselli et al. 2006; Di Stefano et al. 2011; Giacomuzzi et al. 2012; Carannante et al. 2013).

Heat flow is high in southern Tuscany (around 100–200 mW/m^2 in some areas), with peaks of 600 mW/m^2 recorded in the Larderello area, i.e. at the site of the well-known active and long exploited geothermal fields (Della Vedova et al. 1991, 2001, 2006; Minissale 1991; Brogi et al. 2005 with references). Geophysical and field data suggest that much of the heat is provided by partially molten dome-shaped intrusions sited at a minimum depth of about 5000 m (Boccaletti et al. 1997; Gianelli et al. 1997).

CO_2 degassing in southern Tuscany is around 4.8×10^6 mol y^{-1} km^{-2}, about five times the baseline of terrestrial emission (Frondini et al. 2008). Geochemical and isotopic data indicate significant contributions from the upper mantle, as testified by He-isotope signatures of gas manifestations, which show values of $R/R_A = 2.4$ at Orciatico, Montecatini Val di Cecina and Larderello (Minissale et al. 2000).

Tuscany hosts an important metallogenic province that is related to magmatism (e.g. Tanelli and Lattanzi 1986; Dini 2003). Main mineralized districts occur at Elba, in the hilly area of southwestern Tuscany known as “Colline Metallifere”, and at Monte Amiata. Important quantities of iron, lead, copper, zinc, silver, antimony, mercury, and gold, have been extracted from Etruscan times until a few decades ago when mines were closed.

2.3 Composition and Classification of Tuscany Magmatism

The igneous activity of the Tuscany Province emplaced a wide variety of intrusive and extrusive bodies. Volcanic and dike rocks mostly fall in the fields of shoshonite, latite dacite-trachydacite, and rhyolite (Fig. 2.2a). Plutonic rocks partially overlap volcanic compositions, but show moderate enrichment in potassium and mostly concentrate in the acidic field. They span the alkali feldspar granite to diorite field, according to Q’-ANOR classification scheme of Streckeisen and Le Maitre (1979); granodiorites and monzogranites are largely dominating rock types, whereas mafic samples exclusively occur as microgranular enclaves within plutonic rocks (Fig. 2.2b). Several acid intrusive and extrusive rocks show a peraluminous character (Alumina Saturation Index, ASI[1] > 1)

Mafic rocks are mostly represented by dikes, lavas, and enclaves. They are generally saturated to oversaturated in silica, and show variable enrichments in potassium and K_2O/Na_2O ratios, from calcalkaline to ultrapotassic (Fig. 2.2c). An overview of Tuscany rock compositions is shown by variation diagrams reported in Fig. 2.3. These highlight a wide range of major and trace element abundances, with mafic rocks showing very high concentrations of Cr, Ni and Co, typical of unmodified mantle-derived magmas.

Sr–Nd–Pb–Hf isotope ratios display partially overlapping range of values for the silicic and mafic rocks, and all are closer to crustal than to mantle compositions (Fig. 2.4; Vollmer 1977; Hawkesworth and Vollmer 1979; Conticelli et al. 2002, 2010; Gasperini et al. 2002; Farina et al. 2010). This is obvious for the silicic rocks but is rather surprising for the mafic magmas.

[1]Molar ratio of $Al_2O_3/(CaO + K_2O + Na_2O)$.

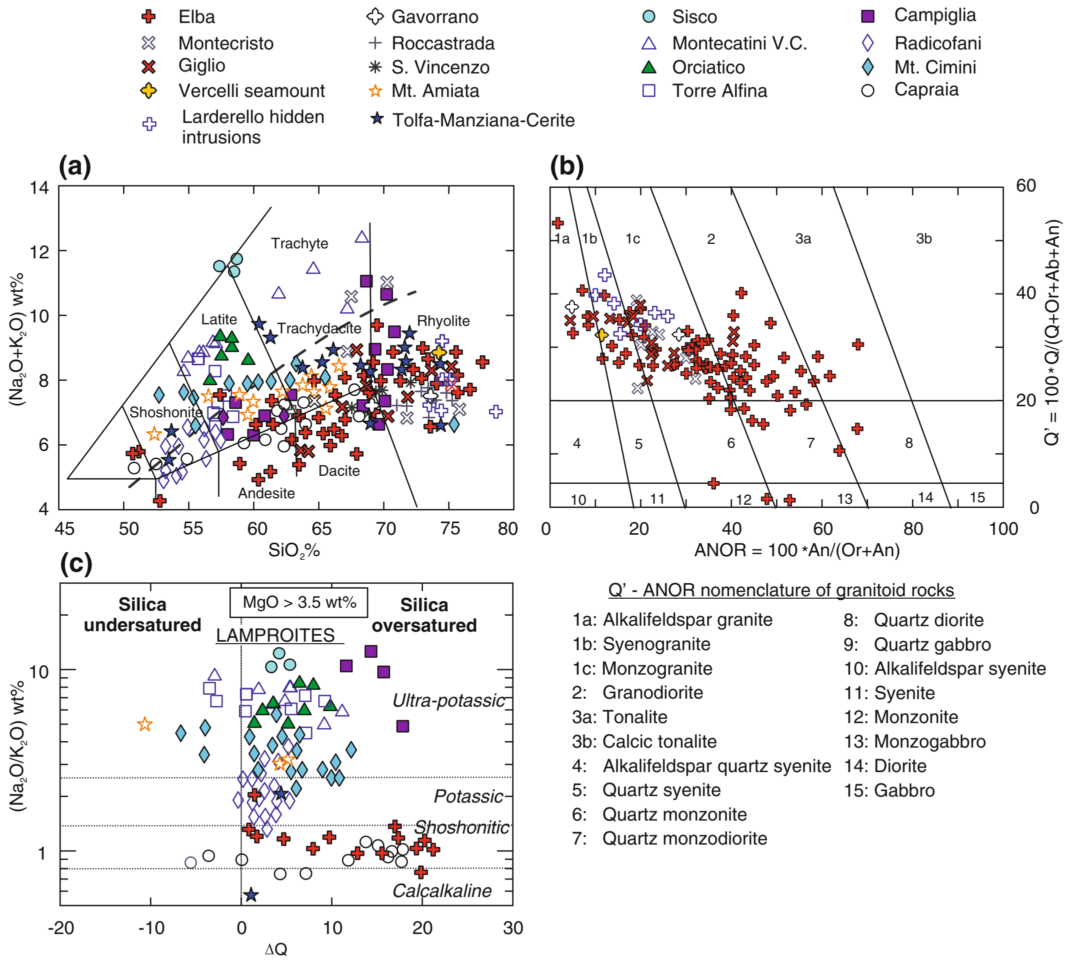

Fig. 2.2 **a** Total-Alkali versus Silica (TAS) classification diagram of Tuscany igneous rocks (Le Maitre 2002). Data recalculated to 100 % on a LOI-free basis. Note that TAS nomenclature applies to volcanic and hypabyssal rocks only. The *dashed line* divides the subalkaline and alkaline fields (Irvine and Baragar 1971). A limited number of representative samples are reported in this and the following plots, to avoid excessive symbol crowding; **b** Q′ versus ANOR classification diagram of Tuscany plutonic rocks; Q, Or, Ab, and An are CIPW normative contents of quartz, orthoclase, albite and anorthite (Steckeisen and Le Maitre 1979); **c** K_2O/Na_2O wt% versus ΔQ diagram for mafic rocks (MgO > 3.5 wt%). ΔQ is the algebraic sum of normative quartz, minus undersaturated minerals (foids and Mg-olivine). Silica undersaturated magmas have ΔQ < 0, whereas oversaturated magmas have ΔQ > 0

Therefore, the Tuscany Magmatic Province is a petrologically anomalous area, where mafic magmas (and their mantle sources) look like the upper continental crust, for radiogenic isotope ratios. Such a statement also applies to incompatible trace elements, as it will be demonstrated later in this chapter.

2.4 Silicic Magmatism

The silicic rocks of the Tuscany province occur as intrusive, hypabyssal and extrusive bodies. Intrusive rocks crop out essentially in the islands of the Tuscan Archipelago (Elba, Montecristo, Giglio), whereas they occur mainly as hidden

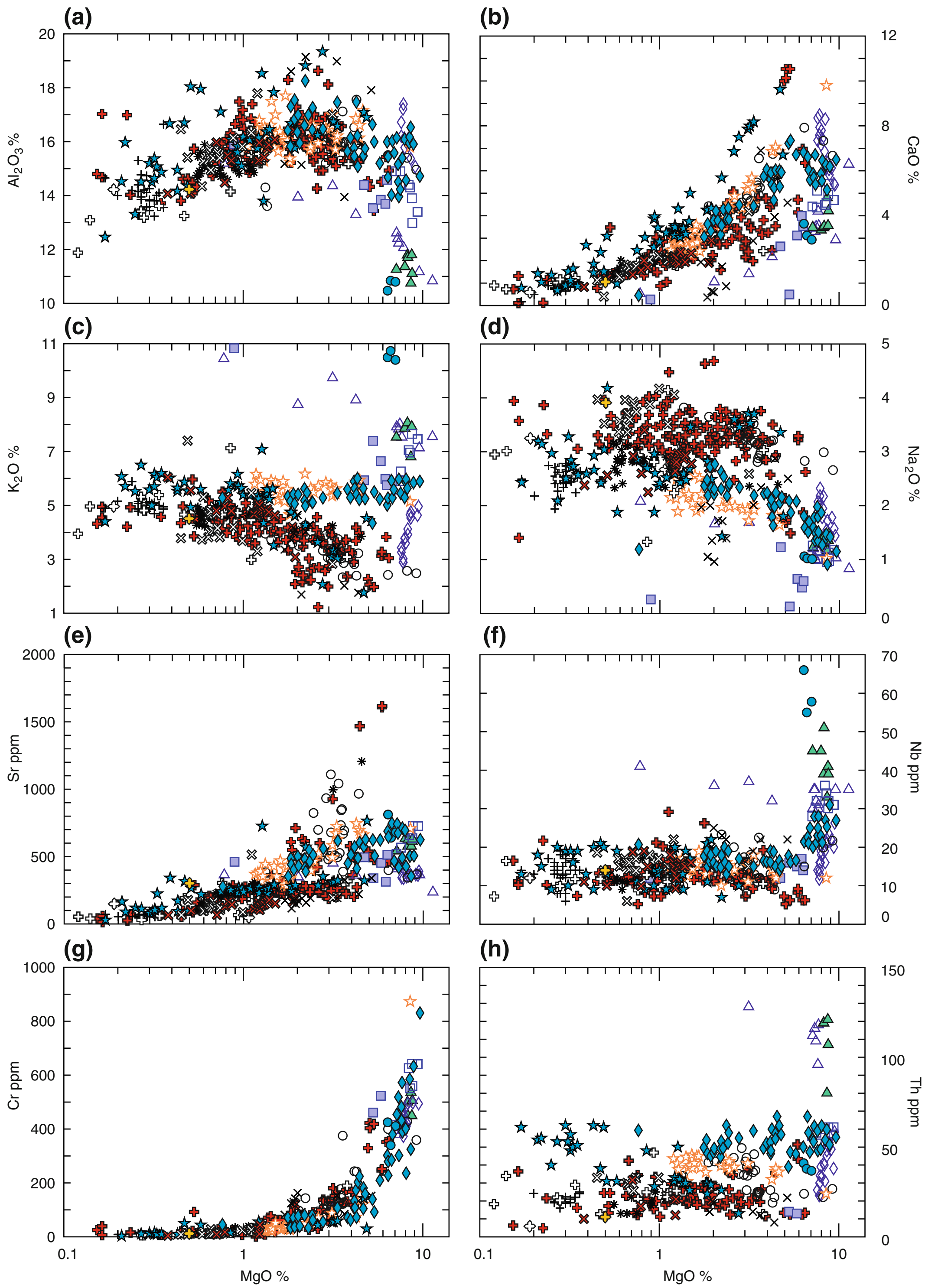

Fig. 2.3 Variation diagrams of selected major and trace elements versus MgO for magmatic rocks of the Tuscany Province. Only selected representative samples from different centres are plotted. Symbols as in Fig. 2.2

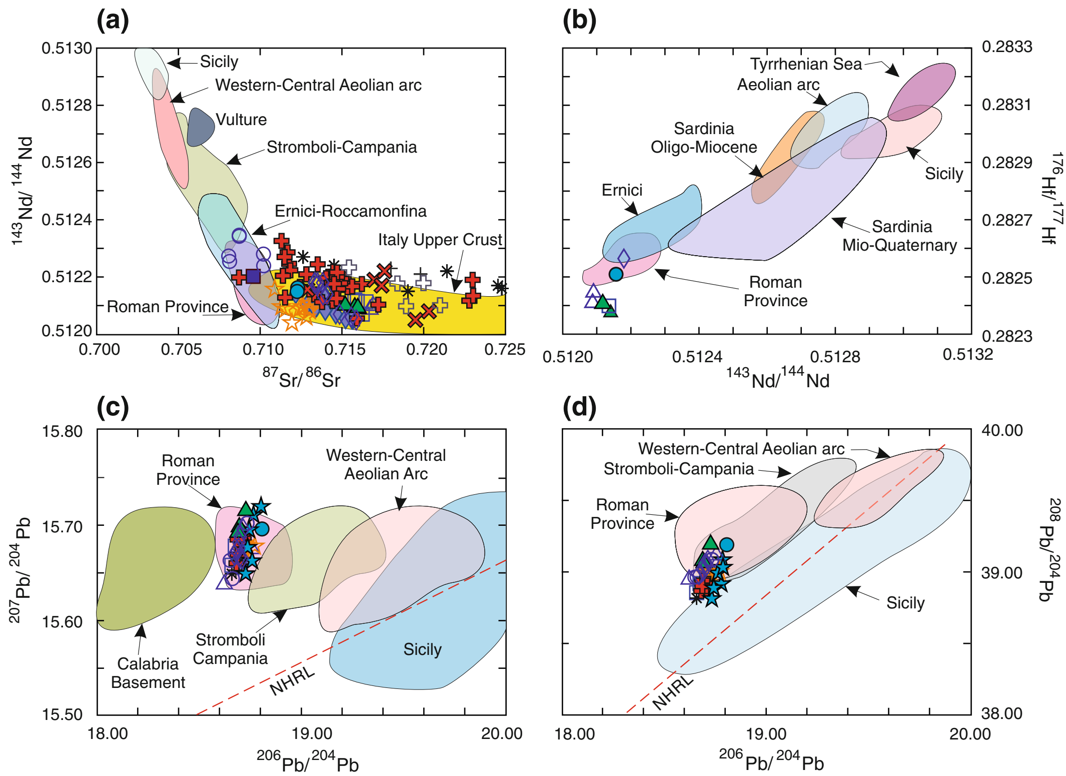

Fig. 2.4 Plots of Sr, Nd, Pb and Hf isotopes of Tuscany magmatic rocks. Compositions of other magmatic provinces (restricted to mafic compositions) from central-southern Italy are shown for comparison. Symbols as in Fig. 2.2

bodies beneath the surface in the mainland of southern Tuscany (e.g. Colline Metallifere, Larderello and Amiata areas). Some seamounts in the northern Tyrrhenian Sea are made of granitoid rocks (e.g. Vercelli; Barbieri et al. 1986; Savelli 2000; Cocchi et al. 2015). Extrusive rocks consist essentially of lava domes and flows, whereas pyroclastic rocks occur only in a few places. Main volcanic silicic centres include San Vincenzo, Roccastrada, Tolfa-Manziana-Cerveteri area and Monte Amiata. Silicic lavas and ignimbrites erupted during the early phases of activity at Cimini volcano where, however, mafic rocks are the most interesting magma types. A few dacites crop out at Capraia, and trachyte veinlets are found within the Montecatini Val di Cecina minette.

2.4.1 Effusive Rocks

San Vincenzo. Rhyolitic lava flows and dome (about 4.5 Ma; Feldstein et al. 1994) crop out at San Vincenzo, on the Tyrrhenian coast of southern Tuscany. Rocks form a small plateau that covers an area of about 10 km^2.

Petrography and mineralogy. Rock texture is porphyritic with phenocrysts of K-feldspar, quartz, plagioclase and biotite, and minor cordierite. Zircon, apatite, epidote, monazite are present as accessories; the groundmass is glassy to microcrystalline. Metasedimentary xenoliths are present in the rhyolites; latite enclaves, megacrysts of diopside ($En_{48}Fs_6Wo_{46}$) and glomeroporphyric aggregates of clinopyroxene, orthopyroxene ($En_{78}Fs_{18}Wo_4$), plagioclase

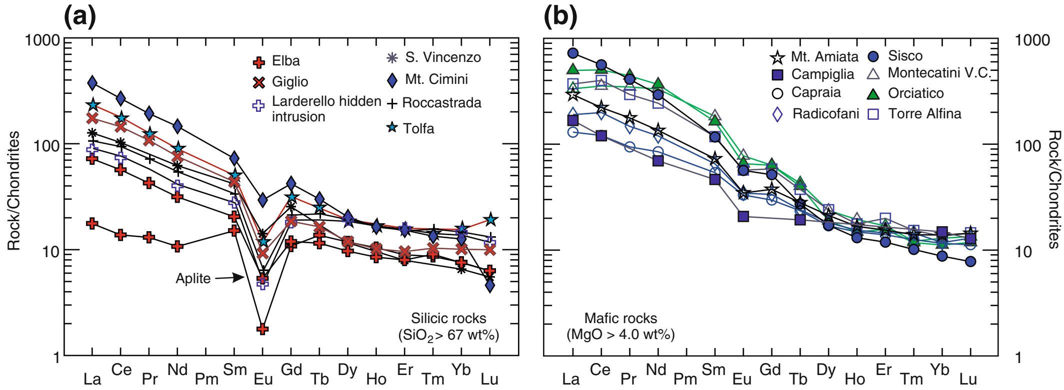

Fig. 2.5 REE patterns of selected silicic **a** and mafic **b** rocks from Tuscany. Normalising values are from Sun and McDonough (1989)

($\sim An_{85\text{-}45}$) and biotite are found in some lavas. Plagioclase phenocrysts are strongly zoned (about An_{80} to An_{30} from core to rim), with the highest anorthite contents being found in the rocks that contain latite enclaves. Alkali feldspar ($Or_{56–78}$) shows minute inclusions of biotite and plagioclase. Biotite occurs as phenocryst and groundmass phase in the rhyolites and in the latite enclaves. Composition is variable (Mg#[2] $\sim$ 0.38–0.78), with maximum Mg# being found in biotites from enclaves (Poli and Perugini 2003a). Cordierite occurs as both euhedral magmatic (Mg# = 0.47–0.59) and anhedral restitic crystals (Pinarelli et al. 1989; Ridolfi et al. 2014).

Petrology and geochemistry. The San Vincenzo rhyolites are peraluminous (ASI = 1.1–1.3), and exhibit important variations for many geochemical parameters. Based on Sr absolute abundances and Sr-isotope ratios, two groups of rocks have been distinguished (Ferrara et al. 1989; Pinarelli et al. 1989). One group of rhyolites, mostly coming from the western sector of the plateau, has relatively lower Sr abundance (Sr $\sim$ 100–150 ppm), and higher initial Sr isotope ratios ($^{87}Sr/^{86}Sr \sim 0.7190–0.7248$) than the rhyolites from the eastern plateau (Sr $\sim$ 200–300 ppm; $^{87}Sr/^{86}Sr \sim 0.7126–0.7154$). Nd isotope ratio ($^{143}Nd/^{144}Nd \sim 0.51215–0.51227$) increases from low-Sr to high-Sr group. Pb-isotope ratios are poorly variable ($^{206}Pb/^{204}Pb \sim 18.66–18.74$; $^{207}Pb/^{204}Pb \sim 15.65–15.68$; $^{208}Pb/^{204}Pb \sim 38.82–38.95$) (Vollmer 1976, 1977; Ferrara et al. 1989; Cadoux et al. 2007). Latite enclaves and pyroxene clots only occur in the high-Sr rhyolites and show high Sr abundances (Sr $\sim$ 1000–1500 ppm), relatively low initial Sr isotope ratio ($^{87}Sr/^{86}Sr \sim 0.7081–0.7088$) and high $^{143}Nd/^{144}Nd$ in the range 0.51245–0.51252; Ferrara et al. 1989; Feldstein et al. 1994). $\delta^{18}O_{SMOW}$ of whole rocks and separated quartz and feldspar ranges from +11.7 to +14.6 ‰ (Turi and Taylor 1976; Masuda and O'Neil 1994). Data for separated phases highlight marked Sr- and O-isotope disequilibrium. REE have variable abundances, increasing from the low-Sr to the high-Sr group, and show fractionated patterns with negative Eu anomalies (Fig. 2.5a).

Petrogenesis. Geochemical and isotopic data on whole rocks, enclaves and separated minerals indicate that the San Vincenzo rhyolites are mixtures between crustal anatectic and mafic-intermediate magmas. Crustal anatectic melts are represented by low-Sr rocks, whereas the mafic end-members had a composition close to that of the latitic enclaves (Ferrara et al. 1989; Pinarelli et al. 1989; Feldstein et al. 1994). Such a mixing process is well highlighted by the hyperbolic trend defined by the San Vincenzo rocks on $^{87}Sr/^{86}Sr$ versus Sr diagram (Fig. 2.6).

[2]Mg# is the molar ratio of MgO/(MgO + FeO).

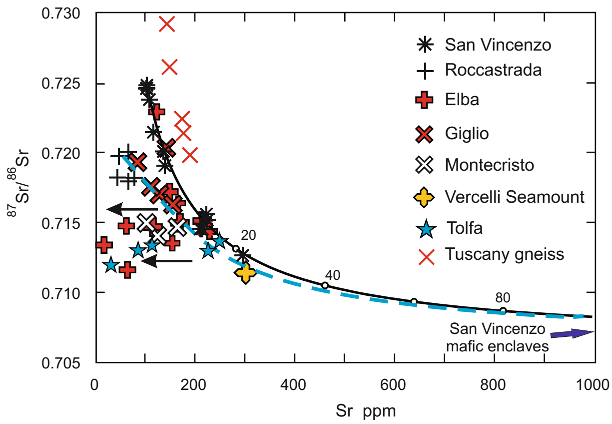

Fig. 2.6 $^{87}Sr/^{86}Sr$ versus Sr for Tuscany silicic rocks. The full line is a mixing trend between the most radiogenic San Vincenzo rhyolite and average mafic enclave from the same centre. Numbers along the line indicate the amounts of mafic melt involved in the mixing. The *blue dashed line* is a mixing trend between Roccastrada rhyolites and San Vincenzo average enclave. *Thin arrows* indicate fractional crystallisation trends. For further explanation, see text

Roccastrada. Rhyolitic lava flows and domes with an age of about 2.5 Ma (Laurenzi et al. 2007) crop out over an area of about 100 km^2 at Roccastrada (Mazzuoli 1967; Pinarelli et al. 1989).

Petrography and mineralogy. The Roccastrada rocks exhibit porphyritic textures with phenocrysts and megacrysts of K-feldspar ($\sim Or_{60-75}$) and quartz, plus minor plagioclase (mostly in the range $An_{50\text{-}20}$), biotite (Mg# $\sim$ 0.50–0.40) and cordierite (Mg# $\sim$ 0.50–0.40). Accessory phases include zircon, apatite, magnetite, and rare garnet. Groundmass texture is generally massive, glassy to perlitic, sometimes microcrystalline. Small xenoliths of metasedimentary origin have been found, whereas there is no evidence for the occurrence of magmatic mafic enclaves.

Petrology and geochemistry. The Roccastrada rhyolites are more strongly peraluminous (ASI $\sim$ 1.2–1.5), richer in silica and Rb and more depleted in Sr and Ba than the San Vincenzo lavas. Composition resembles closely some hidden granites sampled by drilling in the Larderello area (Dini et al. 2005). Radiogenic-isotope signatures are less variable than at San Vincenzo ($^{87}Sr/^{86}Sr \sim 0.7182$–$0.7198$; $^{143}Nd/^{144}Nd \sim 0.51222$; $^{206}Pb/^{204}Pb \sim 18.70$; $^{207}Pb/^{204}Pb \sim 15.67$; $^{208}Pb/^{204}Pb \sim 38.97$; Vollmer 1976, 1977; Hawkesworth and Vollmer 1979; Cadoux et al. 2007). Oxygen isotopic ratio is high with $\delta^{18}O_{SMOW} \sim +13$ ‰ (Turi and Taylor 1976).

Petrogenesis. The Roccastrada rhyolites are considered as pure crustal anatectic magmas. They formed by melting of metasedimentary rocks of the Tuscany basement (e.g. Paleozoic garnet micaschists) and experienced little or no interaction with mafic magmas (Pinarelli et al. 1989; Poli and Perugini 2003b). Lower Sr isotopic ratios than the low-Sr San Vincenzo rhyolites suggest an isotopically less radiogenic source for Roccastrada.

Tolfa-Manziana-Cerite volcanoes. This volcanic complex is the most southerly exposure of the Tuscany Province. It consists of a series of lava domes containing mafic magmatic enclaves and crustal xenoliths, associated with strongly altered pyroclastic flow deposits (Cimarelli and De Rita 2006a). K/Ar ages of 3.7–1.8 Ma were reported by Clausen and Holm (1990), but more restricted values around 3.5 Ma were found for separated sanidine by Villa et al. (1989).

Petrography and mineralogy. The volcanic rocks from Tolfa-Manziana-Cerite range from trachydacite to rhyolite; magmatic enclaves are shoshonites and latites (Clausen and Holm 1990;

Pinarelli 1991; Bertagnini et al. 1995). Trachydacites have a porphyritic texture with phenocrysts of plagioclase (~$An_{60–50}$), sanidine, orthopyroxene (En_{52}), augite and biotite (Mg# = 0.57–0.60) set in a glassy groundmass (De Rita et al. 1994, 1997). Rhyolites are porphyritic with phenocrysts of reversely zoned plagioclase (~$An_{35–70}$), sanidine, and some orthopyroxene and quartz set in a microcrystalline to glassy groundmass. Accessory minerals include zircon, apatite and Fe–Ti oxides. Mafic enclaves have rounded shapes and diffused contacts with the host rocks, indicating they were incorporated in the host magmas still in a molten state. They are porphyritic and contain plagioclase (~$An_{66–52}$), alkali feldspar (~$Or_{54–75}$), diopside to augite clinopyroxene, othopyroxene (~$En_{55–45}$) and biotite (Bertagnini et al. 1995).

Petrology and geochemistry. The Tolfa-Manziana-Cerite rocks are moderately to highly silicic (SiO_2 ~ 63–74 wt%). Mafic enclaves display broadly calcalkaline to potassic alkaline compositions. There is a continuous decrease in Al_2O_3, TiO_2, FeO, MgO and CaO, and an increase in some incompatible elements (e.g. Rb, Th) from mafic enclaves to rhyolites. Isotopic compositions of lavas and pyroclastics are moderately variable ($^{87}Sr/^{86}Sr$ = 0.7123–0.7144; $^{206}Pb/^{204}Pb$ = 18.72–18.75; $^{207}Pb/^{204}Pb$ = 15.65–15.70; $^{208}Pb/^{204}Pb$ = 38.79–38.91; Clausen and Holm 1990; Pinarelli 1991). Mafic enclaves show a somewhat larger range of Sr–Pb isotopic ratios ($^{87}Sr/^{86}Sr$ = 0.7079–0.7127; $^{206}Pb/^{204}Pb$ = 18.72–18.79; $^{207}Pb/^{204}Pb$ = 15.67–15.79; $^{208}Pb/^{204}Pb$ = 38.87–39.12). Metasedimentary xenoliths have much more radiogenic Sr isotope ratios ($^{87}Sr/^{86}Sr$ ~ 0.726; Pinarelli 1991)

Petrogenesis. According to Clausen and Holm (1990), the Tolfa-Maziana-Cerite volcanics were generated by fractional crystallisation starting from intermediate parents, which derived directly from melting of subducted upper crustal rocks. Pinarelli (1991) suggests an origin by melting of metasedimentary crustal rocks followed by fractional crystallisation and mixing with various types of mantle-derived mafic magmas, represented by mafic enclaves. These are derived from anomalous metasomatic mantle sources less strongly enriched in incompatible elements than that of the nearby Roman Province (Pinarelli 1991; Bertagnini et al. 1995).

Monte Amiata. This is a 1738 m-high volcano dominated by trachydacitic lava flows and domes with a few late-erupted shoshonites and latites. The volcano is affected by numerous faults, related either to strike-slip regional tectonics (Brogi et al. 2010) or/and to volcanic spreading over its substratum (Borgia et al. 2014). The high elevation is related to both the accumulation of volcanic products around a central crater area and to doming by magma intrusion in an extensional setting (Acocella and Mulugheta 2001; Marroni et al. 2015). K/Ar and $^{40}Ar/^{39}Ar$ ages range from about 0.4 to 0.2 Ma (see Laurenzi et al. 2015) with a most probable age of 0.3 Ma (Cadoux and Pinti 2009). Well-known and long-exploited cinnabar mineralisations occur at Monte Amiata (Mazzuoli and Pratesi 1963; Barberi et al. 1971; Conticelli et al. 2015b with references).

Petrography and mineralogy. The Monte Amiata trachydacites exhibit a porphyritic texture with abundant phenocrysts and megacrysts of sanidine (~Or_{80}), plagioclase (~$An_{80–50}$), orthopyroxene (~$En_{55–40}$), high-Ti biotite and diopside to augite clinopyroxene. Groundmass is glassy and contains microlites of clinopyroxene, rare orthopyroxene, and some biotite. Xenocrysts of olivine have been observed. Accessory phases include apatite, zircon, ilmenite, magnetite and perrierite, a hydrous sorosilicate of Ca, Fe, Ti, Th and REE (Cristiani and Mazzuoli 2003; Conticelli et al. 2015b with references). Latites and shoshonites are porphyritic with phenocrysts of reversely zoned plagioclase, diopside, and olivine (up to Fo_{90}), set in a hypocrystaline groundmass containing the same phases plus sanidine and glass. Abundant magmatic mafic enclaves and metamorphic xenoliths occur in the Monte Amiata lavas. Mafic enclaves are particularly abundant in the summit domes (van Bergen et al. 1983; van Bergen and Barton 1984; Conticelli et al. 2015b with references), and show clear textural evidence (rounded shapes, chilled margins, etc.) of being incorporated into the host magma when they were still in a molten state (Conticelli et al. 2010, 2015b). Textures are porphyritic with dominant diopside phenocrysts plus some phlogopite-biotite and olivine ($\sim Fo_{90-82}$) set in a groundmass consisting of sanidine, clinopyroxene, biotite and rare olivine. Xenocrysts of plagioclase, sanidine and orthopyroxene are also present (van Bergen et al. 1983).

Petrology and geochemistry. The Monte Amiata lavas have a potassic petrochemical affinity, with the most mafic samples being ultrapotassic in composition (K_2O/Na_2O wt % > 2.5). All samples, except some enclaves, are oversaturated in silica. There is a decrease in FeO_{total}, MgO, CaO, ferromagnesian trace elements, Sr and Ba with increasing silica. In contrast, incompatible elements (e.g. Th, Rb, Nb) remain virtually constant and are rather scattered in the silicic rocks. $^{87}Sr/^{86}Sr$ ratio ($\sim$0.7116–0.7131 for the lavas and 0.7105–0.7118 for the magmatic enclaves) increases linearly with silica, whereas Nd- and Pb-isotopes are poorly variable ($^{143}Nd/^{144}Nd \sim 0.5121$; $^{206}Pb/^{204}Pb \sim 18.71$–18.77; $^{207}Pb/^{204}Pb \sim 15.67$; $^{208}Pb/^{204}Pb \sim 38.98$–39.00; Giraud et al. 1986; Cadoux et al. 2007; Cadoux and Pinti 2009; Conticelli et al. 2015b with references).

Petrogenesis. An origin by mixing between crustal anatectic melts and mafic potassic alkaline magmas similar to the nearby Vulsini district has been suggested by some authors (van Bergen 1985; Peccerillo et al. 1987; Cadoux and Pinti 2009). According to Conticelli et al. (2010), the early-erupted silicic magmas derived from a shoshonitic mafic parent by fractional crystallization plus crustal contamination. The intermediate and final magmas are hybrids between early-erupted high silica magmas and ultrapotassic silica-undersaturated Roman-type melts.

Monti Cimini. This volcano contains significant amounts of early-erupted silicic rocks (trachyte and trachydacite), along with late mafic latite, olivine-latite and shoshonite lavas, which represent the petrologically most important products. Both silicic and mafic rocks are described in Section 2.5.

2.4.2 Plutonic Rocks

Island of Elba. A large number of intrusive bodies crop out in the Island of Elba, showing various size and composition, from monzogranite and granodiorite to alkali-feldspar granite, aplite, and pegmatite. K/Ar, $^{40}Ar/^{39}Ar$, Rb/Sr and U/Pb ages range from about 8.4 to 6.4 Ma (Poli et al. 1989a; Dini et al. 2002; Rocchi et al. 2002, 2003a; Pandeli et al. 2006; Farina et al. 2010; Poli and Peccerillo 2016). A 5.8 Ma old strongly altered shoshonitic mafic dike has been found at Monte Castello, eastern Elba (Conticelli et al. 2001). Fe–Pb–Sn mineralisation are associated with intrusive magmatism at Elba and have been exploited since Etruscan times until a few decades ago. Except for a few intrusions cropping out in the eastern Elba (Monte Castello dikes and Porto Azzurro granites and associated aplites; Conticelli et al. 2001; Pandeli et al. 2006; Dini et al. 2009; Poli and Peccerillo 2016), the igneous activity is concentrated in the western and central sectors of the island, where the magmatism started with intrusions of a series of laccoliths (Capo Bianco aplite, Portoferraio and San Martino porphyries) that emplaced as separate sheets to form a sort of Christmas-tree structure (Rocchi et al. 2002, 2010; Westerman et al. 2004). This was uplifted and displaced laterally by the emplacement of the Monte Capanne monzogranite stock. Dark coloured dikes (Orano porphyries) represent the final stages of the magmatism in this sector of the island.

Petrography and mineralogy. Textures and modal mineralogy of igneous rocks at Elba differ considerably. The Capo Bianco aplites are white-coloured porphyritic alkali-feldspar granites, locally spotted with dark blue spherical aggregates of tourmaline microcrysts. Portoferraio porphyries are monzogranitic to syenogranitic in composition and show a porphyritic texture with phenocrysts of alkali feldspar, quartz, plagioclase and biotite. San Martino monzogranite porphyries are characterised by alkali feldspar megacrysts plus quartz, plagioclase and biotite phenocrysts. Orano dikes consist of monzodiorites to monzogranites containing phenocrysts of plagioclase, biotite and

Fig. 2.7 Mafic enclaves in the Monte Capanne (Elba) monzogranitic rocks. Photo by G. Poli

rare amphibole set in a fine-grained groundmass. The Monte Capanne monzogranitic stock (about 10 km in diameter) is the largest intrusion and is surrounded by a well-developed thermometamorphic aureole. It exhibits a porphyritic texture with various amounts of centimetre- to decimetre-sized euhedral megacrysts of K-feldspar that are set in a medium- to coarse-grained matrix formed of plagioclase, quartz, K-feldspar and biotite with accessory apatite, zircon, thorite, allanite, monazite, ilmenite, and tourmaline. The intrusion contains abundant centimetre- to metre-sized microgranular calcalkaline-shoshonitic mafic enclaves (Fig. 2.7), and is cut by aplitic and pegmatitic dikes, and by the Orano porphyry system. Large euhedral crystals of quartz, K-feldspar, tourmaline, pollucite and other rare minerals have been recovered from pegmatites (e.g. Tanelli and Poggi 2012). Sedimentary and metasedimentary xenoliths, and microgranular mafic enclaves are found in many intrusions (e.g. Farina et al. 2012).

Petrology and Geochemistry. Major and trace element compositions of igneous rocks at Elba are very variable (Fig. 2.3). Capo Bianco aplites show the highest ASI ($\sim$1.3–1.6) and the lowest abundances of TiO_2, FeO_{total}, MgO and CaO among the Elba intrusions. Portoferraio porphyries are richer in TiO_2, FeO_{total}, MgO, CaO than Capo Bianco aplite, a trend that continues in the San Martino porphyries and Monte Capanne monzogranites, up to the Orano porphyries and the late mafic intrusions of eastern Elba. Some Orano dikes show strong enrichments in Sr, Ba and LREE (Fig. 2.3e), but not for other incompatible elements, resembling some andesitic lavas from Capraia and the San Vincenzo mafic enclaves (Poli and Peccerillo 2016). REE decrease slightly with silica and show fractionated patterns with negative Eu anomalies, which are stronger in the aplites (Fig. 2.5a). Sr-isotope ratios of main intrusions are in the range $^{87}Sr/^{86}Sr \sim 0.711–0.723$, increasing from Orano porphyries to the felsic dikes of Cotoncello, an outcrop sited at the northern border of Monte Capanne. A larger range ($^{87}Sr/^{86}Sr \sim 0.7101$–0.7324) has been found for separated phases by Farina et al. (2014). Nd- and Pb-isotope ratios are less variable ($^{143}Nd/^{144}Nd \sim 0.51219$–0.51238; $^{206}Pb/^{204}Pb \sim 18.68$–18.75; $^{207}Pb/^{204}Pb \sim 15.66$–15.69; $^{208}Pb/^{204}Pb \sim 38.87$–38.96). Mafic microgranular enclaves generally have radiogenic isotope compositions lying within the field of host rocks, probably indicating some isotopic re-equilibration with the enclosing magmas (Poli 1992; Dini et al. 2002); however, lower Sr-isotope ratios ($^{87}Sr/^{86}Sr \sim 0.7093$) have been found for some enclaves (e.g. Gagnevin et al. 2004). The Monte Castello mafic dike has $^{87}Sr/^{86}Sr \sim 0.708$–0.709 (Conticelli et al. 2001).

Petrogenesis. According to most authors (Poli et al. 1989a; Dini et al. 2002; Gagnevin et al. 2004, 2005, 2010), the bulk of Elba magmas was formed by mixing between mafic end-members of ultimate mantle origin and peraluminous silicic melts formed by crustal anatexis. Mafic magmas had a calcalkaline-shoshonitic composition similar to the eastern Elba dikes, whereas the crustal end-member had a composition as the Cotoncello intrusion (e.g. Poli 1992; Gagnevin et al. 2004; Poli and Peccerillo 2016). Other authors (e.g. Farina et al. 2012, 2014) suggest that at least part of the petrological variability of Elba intrusions is primary, i.e. reflects compositions of magmas ascended directly from crustal sources with contrasting metapelitic to metavolcanic compositions. Whatever the case, the Elba magmas, especially Monte Capanne, were affected by significant fractional crystallisation and filter-pressing processes with formation of silicic differentiates (leucogranites, aplites and pegmatites) that show radiogenic Sr-isotope compositions similar to their parent monzogranites and granodiorites (Poli et al. 1989a; Rocchi et al. 2002; Poli and Peccerillo 2016).

Island of Montecristo. This island is situated about 60 km south of Elba, along a N-S trending extensional fault, parallel to the Corsica coast. It consists of a monzogranite stock containing microgranular mafic enclaves, cut by aplite and porphyritic dikes. Age (Rb/Sr) is 7.1 Ma (Innocenti et al. 1997).

Petrography and mineralogy. The Montecristo monzogranites have a porphyritic texture with zoned phenocrysts and/or megacrysts of K-feldspar ($\sim Or_{75-85}$), quartz and plagioclase ($\sim An_{25-20}$) surrounded by a medium-grained matrix formed by the same phases, plus variable amounts of biotite ($X_{Fe} \sim 0.62$–0.65) and accessory apatite, zircon, tourmaline, ilmenite, sphene, allanite, monazite, and rutile. Cordierite has been also observed. Aplite dikes (10–30 cm thick) are rich in tourmaline and contain some muscovite. Porphyritic dikes contain ubiquitous biotite ($X_{Fe} \sim 0.41$–0.59) and plagioclase ($\sim An_{55-40}$) phenocrysts, plus resorbed quartz, alkali-feldspars or magnetite in some outcrops.

Petrology and geochemistry. The Montecristo monzogranites display moderate compositional variation (e.g. $SiO_2 \sim 69$–75 wt%; $K_2O \sim 3.7$–4.8 wt%). Porphyritic dikes have slightly lower silica but remarkably higher K_2O contents than monzogranites. Microgranular mafic enclaves ($SiO_2 \sim 58.5$–70.6 wt%), show a broadly calcalkaline composition (Poli 1992; Innocenti et al. 1997). Initial Sr-isotope ratios of monzogranites are around 0.714–0.715, whereas a porphyritic dike has $^{87}Sr/^{86}Sr = 0.70962$ (Innocenti et al. 1997).

Petrogenesis. The origin of the Montecristo monzogranite is attributed to melting of pelitic crustal sources, followed by mixing with mafic magmas and moderate fractional crystallisation. The porphyritic dikes represent late emplaced batches of magmas characterised by higher potassium enrichment than the main intrusion (Innocenti et al. 1997; Rocchi et al. 2003b).

Island of Giglio. The island consists of a main monzogranitic stock, a small leucocratic monzogranitic body forming the Le Scole islets, and a few sedimentary and metamorphic rocks. Rb/Sr age of intrusive units is about 5 Ma (Westerman et al. 1993). Two main texturally distinct rock types are observed in the monzogranite, respectively representing the core and the margin of the intrusion: the Arenella facies forming the eastern half of the island, and the Pietrabona facies occurring on the western island. Dikes and veins of granites, tourmaline-rich aplites and pegmatites occur in the main intrusion and, to a minor extent, in the Le Scole rocks.

Petrography and mineralogy. The Arenella facies is characterized by isotropic texture with abundant megacrysts of K-feldspar set in a medium-grained homogeneous matrix; the Pietrabona facies is strongly foliated with a preferred orientation of minerals and xenoliths. Modal mineralogy of both rock types consists of plagioclase, K-feldspar, quartz and variable amounts of biotite that decreases from Pietrabona to Arenella facies, plus accessory muscovite, tourmaline, Fe–Ti oxides, apatite, monazite, and zircon. Xenocrystic cordierite, garnet, andalusite, and sillimanite have been also observed. Metamorphic xenoliths and microgranular mafic enclaves are common. The leucocratic monzogranite of Le Scole is weakly porphyritic with K-feldspar megacrysts set in a medium- to fine-grained matrix composed of quartz, plagioclase, alkali feldspar, biotite, tourmaline, and cordierite. No microgranular mafic enclaves are found in the Le Scole rocks.

Petrology and geochemistry. The Giglio rocks display moderately variable major and trace element contents (Fig. 2.3), with the Arenella facies displaying lower FeO, MgO, and higher CaO than Pietrabona. Sr-isotope ratios increase from monzogranites ($^{87}Sr/^{86}Sr = 0.7163–0.7176$) to Le Scole leucocratic rocks ($^{87}Sr/^{86}Sr = 0.7195–0.7203$). $^{143}Nd/^{144}Nd$ ranges from 0.51222 to 0.51205 and shows an opposite tendency. The mafic enclaves have comparable and sometimes lower Sr–isotope compositions than the host rocks ($^{87}Sr/^{86}Sr = 0.7128–0.7172$; Westerman et al. 1993, 2003).

Petrogenesis. The magmatism of the Giglio island is related to distinct petrogenetic and intrusive events. The main monzogranite intrusion is older and results from crustal melting plus mixing with moderate amounts of mafic magmas. Le Scole rocks probably represent pure crustal melts that underwent little or no interaction with mafic magmas.

Campiglia Marittima. The granitoid intrusions at Campiglia Marittima only crop out over a small area at Botro ai Marmi. Exposed rocks show monzogranite to alkalifeldspar granite composition, strongly depleted in Fe by secondary processes and, therefore, extensively mined as row ceramic material (Lattanzi et al. 2001). K/Ar age is around 5 Ma (Rocchi et al. 2003c). Independent of granitoid intrusions, felsic and mafic porphyritic dikes (4.3 Ma old) occur in the area (Barberi et al. 1967). The Botro ai Marmi rocks contain quartz, orthoclase and some plagioclase with scarce altered biotite. Strong alteration by late magmatic fluids affected the intrusion and the surrounding thermo-metamorphic and sedimentary rocks. These processes generated dramatic modification of rock compositions and were responsible for the formation of Cu–Pb–Zn–Ag mineralisation. Least-altered intrusive rocks are moderately peraluminous (ASI $\sim$ 1.2) and silicic ($SiO_2 \sim 70$ wt%).

Gavorrano. Intrusive rocks at Gavorrano consist of about 4.3 Ma old biotite-bearing monzogranite with K-feldspar megacrysts, and tourmaline-rich alkali feldspar granite. The exposed intrusion is about 3 km long and NNW-SSE oriented (Mazzarini et al. 2004; Musumeci et al. 2005). Major and trace element compositions are rather variable (e.g. $SiO_2 \sim$ 66–75 wt%; Rb = 250–700). Except for Rb, incompatible trace element contents and REE fractionation decrease with increasing silica, suggesting separation of accessory phases such as monazite (Poli et al. 1989a; Rocchi et al. 2003c; Dini et al. 2005). Sr-isotope ratios are in the lower range of Tuscany silicic rocks ($^{87}Sr/^{86}Sr = 0.7139–0.7149$; Ferrara and Tonarini 1985), possibly an effect of interaction between crustal anatectic and relatively unradiogenic mantle-derived magmas.

Hidden plutons. There are several hidden intrusions in southern Tuscany, whose presence has been revealed by geophysical investigation and drillings (e.g. Zitellini et al. 1986; Gianelli and Laurenzi 2001). Northeast of Gavorrano (**Castel di Pietra**), borehole drilling encountered 4.3 Ma plutonic rocks at a depth of about 870–880 m beneath a thick thermometamorphic roof

(Franceschini et al. 2000). Cored samples include porphyritic monzogranites, fine-grained leucocratic syenogranites, and orthopyroxenene-bearing dark granodiorites and monzogranites. Silica (SiO_2 ~ 65–72 wt%) and Sr isotope ratios ($^{87}Sr/^{86}Sr$ ~ 0.7145–0.7222) increase from the dark to leucocratic facies (Dini et al. 2003). At **Monte Spinosa**, a few kilometres south of Botro ai Marmi, syenogranites and monzogranites with SiO_2 = 66–71 wt% have been recovered. In the **Larderello** area, a series of borehole drillings (Monteverdi, Radicondoli, Travale, Carboli) encountered peraluminous muscovite-biotite bearing syenogranites to monzogranites with ages of 3.8–1.3 Ma (Gianelli and Laurenzi 2001; Villa et al. 2001; Dini et al. 2005). Mafic enclaves commonly contained by other Tuscany intrusive rocks have not been observed in these granitoids. According to Dini et al. (2005), the hidden intrusions of the Larderello area represent pure crustal anatectic magmas formed by melting of biotite and muscovite-rich metasedimentary sources. However, Sr-isotope ratios are variable and somewhat lower ($^{87}Sr/^{86}Sr$ = 0.7148–0.7209) than the local basement ($^{87}Sr/^{86}Sr$ ~ 0.7196–0.7318), calling for a less radiogenic component of deep crustal or subcrustal origin.

Seamounts: Several seamounts, partly with granitoid composition, occur between Corsica and Tuscany. These are aligned along a north-south trending ridge, south of Elba and Montecristo islands (Savelli 2000), in a zone characterised by a tectonic style that recalls the Basin and Range province (Carmignani and Kligfield 1990; Marani and Gamberi 2004). A sample dredged from the Vercelli seamount, southeast of this alignment near to the 41° Parallel line, revealed a K/Ar age on feldspar of 7.2 Ma, a tourmaline-biotite syenogranite composition, and initial $^{87}Sr/^{86}Sr$ = 0.71140 (Barbieri et al. 1986; Table 2.2). The Vercelli Seamount is a 8 km long and 3.4 km wide, SW-NE oriented edifice, whose summit rises about 1200 m above its surrounds, reaching 58 m bsl. A highly magnetic body, possibly a mafic lava flow, has been detected near to Vercelli (Cocchi et al. 2015).

2.5 Mafic Magmatism

Mafic magmas (MgO higher than 3.5–4.0 wt%) make up small hypabyssal and effusive bodies, the large volcanoes of Capraia and the younger effusive activity of Monti Cimini. They are also present as enclaves and dikes in several silicic intrusive and extrusive rocks, as recalled earlier in this chapter. Compositions range from calcalkaline and shoshonitic to ultrapotassic lamproitic (Fig. 2.2c). Lamproites are slightly undersaturated to oversaturated in silica and show high MgO and SiO_2 abundances and relatively low concentrations of CaO, Al_2O_3, Na_2O, and FeO_{total} (Peccerillo et al. 1988; Conticelli and Peccerillo 1992; Conticelli et al. 2015a). The most primitive calcalkaline and shoshonitic compositions exhibit higher CaO, Na_2O, FeO_{total} and Al_2O_3 than lamproites, as observed for typical calcalkaline basalts, such as those from the Aeolian Islands (Fig. 2.8).

Sisco. A small sill intruded into Alpine high-pressure metamorphic terrains occurs in northeastern Corsica, south and west of Marine de Sisco along the D80 route (Peccerillo et al. 1988; Marinosci 1993). K/Ar ages yielded values from 15.5 to 13.5 Ma (Civetta et al. 1978; Bellon 1981).

Petrography and mineralogy. The rock is a lamprophyre with a slightly porphyritic to microgranular texture, consisting of altered olivine, phlogopite, sanidine (Or_{95}), Al-poor diopside, and K-richterite. Accessory minerals include titanite, chromite, ilmenite, priderite (K–Ba–Fe^{3+}–Ti oxide), rutile and rare roedderite, a cyclosilicate of Fe, Mg, Na, K (Wagner and Velde 1986).

Petrology and geochemistry. The Sisco rock is a peralkaline (Peralkaline Index, PI[3] > 1; normative acmite around 4–5 wt%) high-silica lamproite exhibiting relatively high concentrations of MgO (~6.5–7.0 wt%), Ni (~250 ppm), Co and Cr, and moderate abundances of Sc (~10 ppm) and V (~90 ppm). Al_2O_3 (~10 wt%) and Na_2O

[3]PI (Peralkaline Index) is the molar ratio of (Na_2O + K_2O)/Al_2O_3.

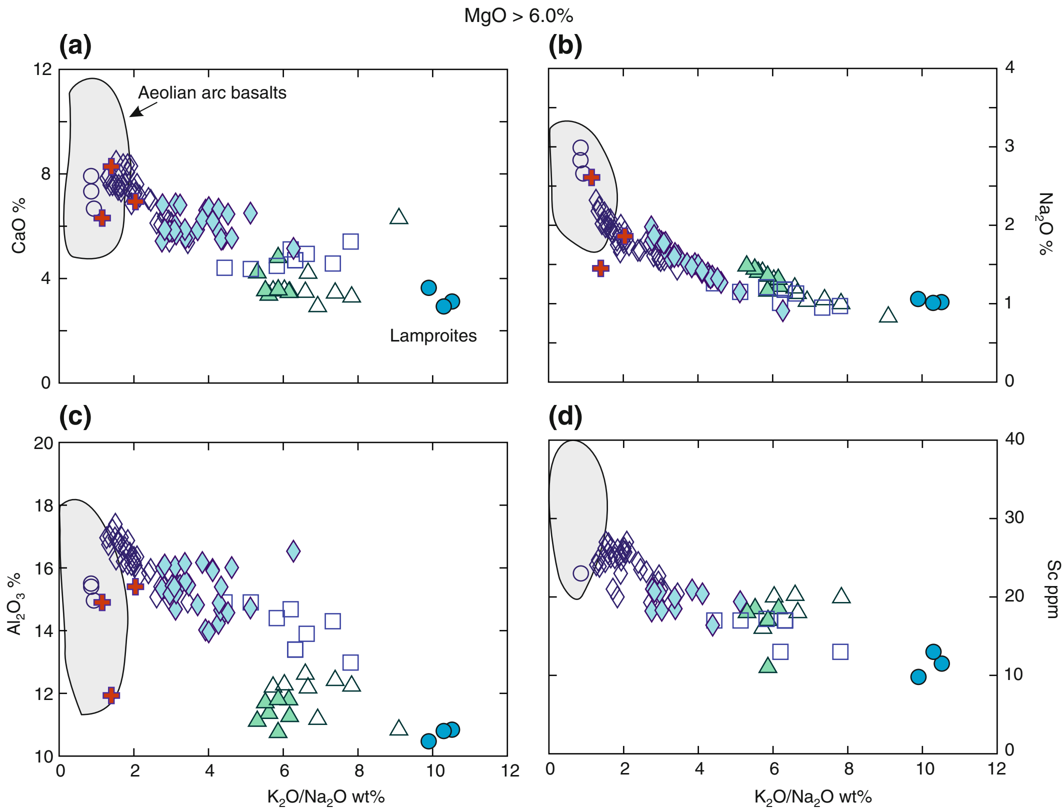

Fig. 2.8 CaO, Na_2O, Al_2O_3, and Sc versus K_2O/Na_2O relationships for the most primitive rocks (MgO > 6.0 wt %) from Tuscany. The field of calcalkaline basalts from the Aeolian arc is reported for comparison (Peccerillo et al. 2013). Symbols as in Fig. 2.2

(~1.0 wt%) are low, a feature that is typical of lamproites. REE are fractionated with a small negative Eu anomaly (Fig. 2.5b). The mantle-normalised incompatible element pattern differs somewhat from those of Tuscany lamproites because of lower enrichments in some LILE (Cs, Rb, Th, U) and the lack of a positive spike of Pb (Fig. 2.9a). The initial Sr isotope ratio is relatively high ($^{87}Sr/^{86}Sr$ ~ 0.7123). Nd, Pb and Hf isotope ratios are poorly to moderately radiogenic ($^{143}Nd/^{144}Nd$ ~ 0.51216; $^{206}Pb/^{204}Pb$ ~ 18.81 $^{206}Pb/^{204}Pb$ ~ 15.69 $^{206}Pb/^{204}Pb$ ~ 39.19; $^{176}Hf/^{177}Hf$ = 0.282504). Initial Os isotope ratio is $^{187}Os/^{188}Os$ = 0.1889 (Conticelli et al. 2007, 2009a, 2010).

Petrogenesis. High MgO, Ni, and Cr abundances clearly indicate a mantle origin for the Sisco lamproite. The low abundances in Al_2O_3 and Na_2O suggest a clinopyroxene-poor harzburgitic source. On the other hand, radiogenic isotope signatures and LILE abundances call for an enriched mantle source, which was affected by metasomatic processes.

Orciatico. The Orciatico outcrop consists of a laccolith several meters thick, and a small vertical feeder dike intruded into Pliocene marly sediments. Glass-rich chilled margins occur at the contact with intruded sediments. Age is 4.1 Ma (Conticelli et al. 1992)

Petrography and mineralogy. Textures are poorly porphyritic with microphenocrysts of olivine (~Fo_{90-75}), phlogopite (Mg# ~ 75–79), and Al-poor diopside (Al_2O_3 ~ 0.5 wt%; Cellai et al. 1994) set in a groundmass consisting of the same phases plus sanidine, glass, and accessory K-richterite, rutile, ilmenite, and Mg-chromite. Some of the high-MgO olivine crystals show evidence of corrosion and kinking, and are

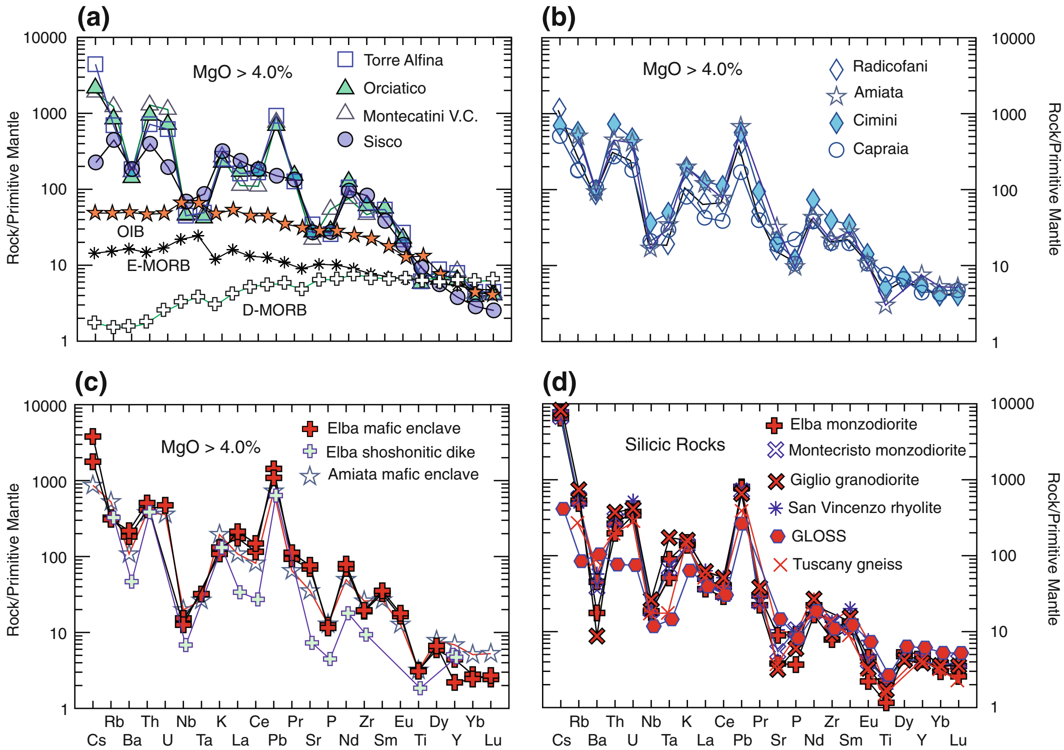

Fig. 2.9 Incompatible element patterns normalised to primordial mantle composition (Sun and McDonough 1989) of representative Tuscany mafic rocks **a**, **b**, of mafic enclaves and shoshonitic dike **c**, and of selected silicic crustal rocks **d**. GLOSS is the average Global Subducted Sediments of Plank and Langmuir (1998); D-MORB, E-MORB, and OIB are averages of depleted and enriched Mid-Ocean Ridge Basalts (Gale et al. 2013) and of Ocean Island Basalts (Sun and McDonough 1989)

probably xenocrysts resulting from disaggregation of high-pressure ultramafic xenoliths (Poli 1985; Wagner and Velde 1986; Peccerillo et al. 1987, 1988; Conticelli and Peccerillo 1992; Conticelli et al. 1992).

Petrology and geochemistry. The Orciatico rocks are high silica lamproites that differ from Sisco, because of a lower peralkaline index (PI ~ 0.9–1.0), K_2O, TiO_2 Nb, and Ta, slightly higher Al_2O_3 and Na_2O, and much higher Cs, Rb, Th, U, and Pb. MgO, Ni, Co, and Cr are in the range of mantle equilibrated melts. The REE pattern is fractionated, with an upward convexity for light REE and a small negative Eu anomaly (Fig. 2.5b). Incompatible element patterns are highly fractionated and contain pronounced positive spikes of Cs, Rb, Th and Pb, and stronger negative anomalies of HFSE than Sisco (Fig. 2.9a). Overall, they closely resemble patterns of some upper crustal rocks such as Tuscany gneiss or crustal anatectic rhyolites (Fig. 2.9d; Peccerillo and Martinotti 2006). Sr–Nd–Pb–Hf–Os isotope ratios are closer to upper crustal than to mantle values, or somewhat intermediate between the two ($^{87}Sr/^{86}Sr$ = 0.7152–0.7159; $^{143}Nd/^{144}Nd$ = 0.5121; $^{206}Pb/^{204}Pb$ = 18.69–18.73; $^{176}Hf/^{177}Hf$ = 0.28240; $^{187}Os/^{188}Os$ = 0.3405; Fig. 2.4; Table 2.2). Oxygen-isotope ratios show large differences between phenocryst and groundmass minerals with $\delta^{18}O_{SMOW}$ ~ +7.2 ‰ in olivine phenocrysts and $\delta^{18}O_{SMOW}$ ~ +11.1 ‰ in groundmass sanidine (Peccerillo et al. 1988; Barnekow 2000; Conticelli et al. 1992, 2007, 2010).

Petrogenesis. The major, trace element and radiogenic isotope signatures of Orciatico lamproite suggest an origin in a mantle source depleted in some major elements (i.e. CaO, Na_2O), but strongly enriched in geochemical components akin to the upper continental crust, such as metapelites.

Montecatini Val di Cecina. The Montecatini subvolcanic body is a 4.1 Ma old plug (Borsi et al. 1967) intruded into Miocene marine and lacustrine sediments and Liguride units. The rock is a phlogopite-rich lamprophyre[4] (minette) permeated by a dense network of leucocratic veinlets.

Petrography and mineralogy. The Montecatini minette has a medium- to fine-grained sometimes porphyritic texture with abundant phlogopite, Al-poor augite (Cellai et al. 1994), K-feldspar, minor altered olivine and accessory apatite, amphibole, Fe–Ti oxides, zircon, thorite, apatite and perrierite (Peccerillo et al. 1988; Conticelli et al. 1992). The leucocratic veinlets consist of dominant sanidine with minor quartz and brown mica, plus accessory apatite. These veinlets likely represent residual melts separated from the host magma during crystallisation.

Petrology and geochemistry. The Montecatini minette has similar major element composition as the Orciatico rock, although the peralkaline index is lower (PI $\sim$ 0.8–0.9) and P_2O_5 is higher. Incompatible element and REE patterns, and Sr–Nd–Pb–Hf–Os isotope ratios are not far from values of Orciatico ($^{87}Sr/^{86}Sr = 0.7169$; $^{143}Nd/^{144}Nd = 0.5121$; $^{206}Pb/^{204}Pb = 18.76$; $^{176}Hf/^{177}Hf = 0.28245$; $^{187}Os/^{188}Os = 0.5502$; Table 2.2). The leucocratic veins have a trachytic composition and similar radiogenic isotopic composition to the host minette (e.g. Peccerillo et al. 1988; Conticelli et al. 1992, 2007, 2010).

Petrogenesis. Similar geochemical compositions and ages of the Montecatini and Orciatico rocks suggest a common origin. Some differences between the two occurrences could result from the separation of felsic veinlets in the Montecatini magma, which somewhat modified the original composition of the lamproitic magma.

[4]The term *lamprophyre* is used in this book to indicate dike rocks characterised by mafic mineral phenocrysts (amphibole, biotite, phlogopite etc.) with feldspar and/or feldspatoids confined in the groundmass. They take different names depending on mineralogy (e.g. Gill 2010).

Torre Alfina. This is a small volcano (about 0.8 Ma old) formed by a few lava units, one of whom is several hundred meters long, and two necks. The Torre Alfina rocks contain a large number of xenoliths of both crustal and mantle origin, which document a rapid magma ascent on the order of few hours (Conticelli and Peccerillo 1990, 1992; Barnekov 2000; Casagli 2009). The xenoliths, best observed on the front wall of the castle dominating the village of Torre Alfina (Fig. 2.10), include large amounts of crustal rocks (granulites, gneiss, schists, sandstones and marls) and a few cm-sized ultramafic nodules (phlogopite-bearing dunites, spinel harzburgites and lherzolites, and rare phlogopite-rich peridotites). Geothermobarometric investigations on ultramafic xenoliths gave equilibration T-P of about 1050 °C and 1.5 GPa, corresponding to a depth of 50–60 km (Pera et al. 2003). Most of the crustal xenoliths and xenocrysts show evidence of partial melting and reaction with the host magma, exhibiting one of the most compelling cases of wall rock assimilation by a rapidly ascending hot mafic magma (Conticelli 1998).

Petrography and mineralogy. Rocks have aphyric to poorly porphyritic texture and the only phenocryst phase is rare euhedral to skeletal Mg-olivine (up to Fo_{92}). Groundmass phases include olivine, low-Al diopside, phlogopite (Mg# $\sim$ 95), K-feldspar (Or_{82-85}), glass and accessory ilmenite, Ti-magnetite and Mg-chromite. The latter is also found as inclusions within olivine phenocrysts (Conticelli 1998).

Petrology and geochemistry. The Torre Alfina lavas have similar composition to the Montecatini and Orciatico lamproites, except for lower Th and Rb contents and higher $^{187}Os/^{188}Os$ (=0.2756; Conticelli et al. 2007). There are small but significant compositional variations between lava flows and necks.

Petrogenesis. A mantle origin for the Torre Alfina magmas is clearly indicated by both rock geochemistry and occurrence of high-P ultramafic xenoliths. The phlogopite-rich peridotite xenoliths found in the lavas could represent the source of the Torre Alfina magma (Conticelli and Peccerillo 1990). Geochemical differences within lava flows and necks have been suggested to derive from

Fig. 2.10 Front wall of the Torre Alfina castle showing large amounts of a wide variety of crustal and mantle xenoliths in the lamproite lavas

assimilation of variable amounts of crustal rocks by ascending magma. Such a process generated minor modification of trace element ratios and isotopic signatures, and a general dilution for several compatible and incompatible elements (e.g. $^{87}Sr/^{86}Sr$ from about 0.7158 to 0.7165, Ni from 350 to 250 ppm; La from 100 to 85 ppm; Conticelli 1998).

Campiglia. Mafic dikes with an age of about 4.3 Ma occur in the Campiglia area, as mentioned earlier in this chapter. These dikes are strongly altered and have porphyritic textures with phenocrysts of clinopyroxene, plagioclase, biotite, alkali feldspar and some corroded quartz set in a groundmass of plagioclase, sanidine, and pyroxene. Major element compositions of least altered samples are characterised by high K_2O and K_2O/Na_2O ratio, resembling high-silica lamproites from Montecatini and Orciatico. However, concentrations of several incompatible elements that are relatively immobile during secondary alteration (e.g. Ti, Nb, LREE, Zr, Hf), as well as Sr isotope ratio ($^{87}Sr/^{86}Sr = 0.7096$) are lower and Nd isotope ratio ($^{143}Nd/^{144}Nd = 0.51220$) is higher at Campiglia, and rather resemble Capraia calcalkaline and shoshonitic rocks (Peccerillo et al. 1987; Conticelli and Peccerillo 1992; Conticelli et al. 2002). This suggests that high enrichments in potassium could be a secondary feature and that the

Campiglia mafic magmas had a calcalkaline to shoshonitic original composition.

Monti Cimini. This is a 1.35–0.94 Ma volcano formed of early trachyte (<20 % normative quartz) and trachydacite (>20 % normative quartz) lava domes, welded ignimbrites and lava flows, followed by latite, olivine-latite and shoshonite lavas (Puxeddu 1971; Lardini and Nappi 1987; Cimarelli and De Rita 2006b; LaBerge et al. 2006; Aulinas et al. 2011; Conticelli et al. 2013 and references therein).

Petrography and mineralogy. Trachytes and trachydacites display porphyritic textures with phenocrysts and megacrysts of sanidine plus plagioclase, biotite, othopyroxene and some clinopyroxene set in a hypocrystalline groundmass containing the same phases plus accessory ilmenite, apatite, zircon, monazite, and perrierite. Latites and shoshonites have aphyric to porphyritic textures with phenocrysts of olivine and minor clinopyroxene set in a groundmass composed of the same phases plus sanidine and accessory chromite, Ti-magnetite and ilmenite. Mineral chemistry is very variable. Olivine ranges from about Fo_{93} to Fo_{40} from phenocryst cores to rims and groundmass and sometimes contain Mg-chromite inclusions; orthopyroxene ranges from enstatite to ferrosilite ($\sim En_{65-45}$), and mica from biotite to phlogopite. Clinopyroxene ranges from augite and diopside to hedenbergite ($Di_{54}Fs_{18}Wo_{28}$, to $Di_{20}Fs_{32}Wo_{46}$ with Mg# = 90–39); their Al_2O_3 content is variable (0.3–7.9 wt%) and minimum values are found in phenocrysts of the most potassic samples, in which Al is not sufficient to fill the tetrahedral site. Ti/Al (>0.2, expressed as atoms per formula unit: afu) of clinopyroxene and Cr/(Cr + Al) of chromite are high (Fig. 2.11) and close to values found in the same phases from Tuscany lamproites (Aulinas et al. 2011; Conticelli et al. 2013).

Petrology and geochemistry. The Monti Cimini rocks have variable K_2O/Na_2O ratio (~2–5), which decreases with silica. Mg#, Ni, Co and Cr of mafic rocks are high and close to values of primary mantle melts and decrease linearly with increasing silica. Notably, several incompatible elements (e.g. Rb, Nb, Zr, Hf) also show a similar trend. The incompatible element patterns normalised to primitive mantle composition resemble those of Tuscany lamproites. Initial Sr- and Nd-isotope ratios are variable ($^{87}Sr/^{86}Sr \sim 0.7122$–0.7157; $^{143}Nd/^{144}Nd \sim$ 0.51205–0.51214), especially in the mafic rocks. Pb isotopic ratios ($^{206}Pb/^{204}Pb$ = 18.69–18.73; $^{207}Pb/^{204}Pb$ = 15.66–15.69; $^{208}Pb/^{204}Pb$ = 38.92–39.02) are not much different from other Tuscany rocks (Aulinas et al. 2011; Conticelli et al. 2013 and references therein).

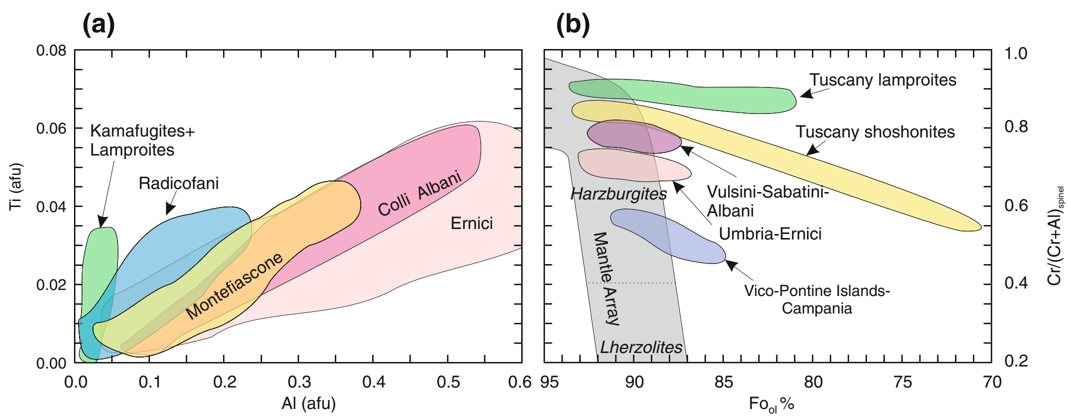

Fig. 2.11 **a** Ti versus Al (atoms per formula units, afu) in clinopyroxenes from some Italy volcanic rocks; **b** Cr/(Cr + Al), atomic ratios of spinel inclusions versus forsterite contents of host olivine for some Italy volcanics. The Mantle Array is from Arai (1994). Redrawn after Nikogossian and van Bergen (2010) and Conticelli et al. (2011, 2013)

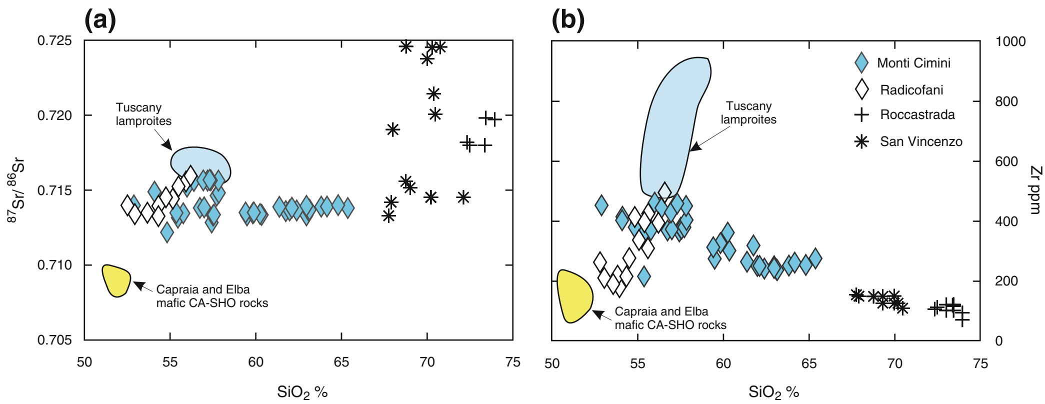

Fig. 2.12 $^{87}Sr/^{86}Sr$ and Zr versus SiO_2 for Monti Cimini and Radicofani rocks

Petrogenesis. The origin of Monti Cimini magmas can be well explained by binary plots of SiO_2 (or MgO) versus $^{87}Sr/^{86}Sr$ and incompatible elements (Fig. 2.12). The most mafic rocks (shoshonites and olivine-bearing latites) plot between the Capraia-Elba calcalkaline-shoshonitic mafic rocks (or also the Roman potassic trachybasalt) and the Tuscany lamproites. In contrast, the more evolved rocks (latites, trachytes and trachydacites) define a distinct trend, which starts from mafic samples and points to silicic compositions such as those of Roccastrada and San Vincenzo rhyolites. These variations suggest that the Cimini mafic magmas were generated either by variable degrees of melting of a heterogeneous mantle source or by mixing between calcalkaline-shoshonitic and lamproitic magmas. The evolved rocks can be explained by mixing between a mafic end-member and crustal anatectic liquids with compositions similar to Roccastrada and San Vincenzo.

Radicofani. The volcano at Radicofani consists of a neck and a few remnants of lava flows with K/Ar and $^{40}Ar/^{39}Ar$ ages clustering around 1.3 Ma (D'Orazio et al. 1991, 1994). In spite of its small size, the Radicofani volcano shows important variations for both geochemistry and mineralogy. Rocks range from basaltic andesite to shoshonite and latite, according to the TAS classification of Le Maitre (2002). Basaltic andesites make up the base of the neck and become more potassium- and silica-rich at the top. Lavas similar to the upper neck crop out at Poggio Sasseta, north of the Radicofani village. Shoshonite lavas occur at the nearby localities of Poggio Casano and Ceppete (D'Orazio et al. 1994).

Petrography and mineralogy. Basaltic andesites at the base of the neck are poorly porphyritic with phenocrysts of plagioclase ($\sim An_{90-80}$), zoned olivine ($\sim Fo_{75-60}$) and augite-diopside clinopyroxene set in a groundmass made of the same phases plus orthopyroxene, ilmenite, sanidine, and accessory biotite, apatite, magnetite and glass (Poli et al. 1984; D'Orazio et al. 1994; Barnekow 2000). A modification in the mineralogy is observed at the top of the neck, where forsterite content of olivine and the modal amount of alkali feldspar in the groundmass increase, whereas plagioclase becomes rare or disappears as a phenocryst phase. Shoshonites are microcrystalline to poorly porphyritic with phenocrysts of olivine ($\sim Fo_{85-70}$) and minor clinopyroxene. Plagioclase is scarce and restricted to the groundmass. This consists of dominant K-feldspar plus Al-poor clinopyroxene, biotite, plagioclase and accessory amounts of olivine, brown amphibole, Fe–Ti oxides, apatite, and glass. Chromite inclusions are common in olivine phenocrysts. The Radicofani volcanics contain a few xenocrystic minerals coming from the wall rocks (corroded quartz and some cordierite) and rare small ultramafic nodules.

Petrology and geochemistry. Major element composition shows poorly variable silica

(SiO_2 ~ 53–56 wt%) and MgO (~8–9 wt%) contents. In contrast, incompatible elements (Rb, Th, Nb, Ta, REE, etc.) and some ferromagnesian elements (Ni, Cr) vary considerably, and are positively correlated with K_2O and SiO_2; in contrast, Na_2O, V, and Sc show a negative trend (D'Orazio et al. 1994; Conticelli et al. 2011). The incompatible element patterns normalised to primordial mantle composition resemble those of Tuscany lamproites, although absolute element enrichment is lower (Fig. 2.9b). $^{87}Sr/^{86}Sr$ ratios (0.7133–0.7159) increase with K_2O and SiO_2, i.e. from basaltic andesites to shoshonites, whereas $^{143}Nd/^{144}Nd$ ratios (0.51205–0.51218) exhibit an opposite trend (D'Orazio et al. 1994; Conticelli et al. 2002). Pb- and Hf-isotope ratios ($^{206}Pb/^{204}Pb$ ~ 18.67–18.72; $^{207}Pb/^{204}Pb$ ~ 15.66–15.69; $^{208}Pb/^{204}Pb$ ~ 38.98–39.08; $^{176}Hf/^{177}Hf$ = 0.28255) fall in the field of the Tuscany ultrapotassic rocks (De Astis et al. 2000a, b; Conticelli et al. 2002; Gasperini et al. 2002). O-isotopes on clinopyroxene and olivine vary from $\delta^{18}O_{SMOW}$ = +6.9 to + 7.8 ‰ (Barnekow 2000).

Petrogenesis. Overall, the compositions of Radicofani magmas are intermediate between moderately potassic rocks such as those from Capraia or some Roman-type trachybasalts, and lamproites (Fig. 2.12). This suggests an origin by mixing between magmas with contrasting calcalkaline-shoshonitic and lamproitic compositions. Such a hypothesis is supported by the variable Ti/Al of clinopyroxenes that encompass lamproitic and Roman-type compositions (Fig. 2.11a). Conticelli et al. (2011) reject the magma mixing hypothesis and suggest that compositional variation is related to melting of a veined lithospheric mantle, with variable contribution from veins and host peridotite.

Island of Capraia. This is the only volcano in the Tuscany Province dominated by calcalkaline rocks. The island was constructed during two distinct phases of activity at about 7.6–7.2 Ma and 4.6 Ma (Borelli et al. 2003; Gasparon et al. 2009). The older phase is dominated by lavas, which make up the bulk of the island. They show intermediate composition and are classified as high-K calcalkaline andesites and dacites, according to the classification scheme of Peccerillo and Taylor (1976). Younger activity is represented by the shoshonitic basalts of Punta dello Zenobito, a monogenetic strombolian centre at the southernmost end of the island (Prosperini 1993; Borelli et al. 2003; Poli and Perugini 2003c).

Petrography and mineralogy. The shoshonitic basalts from Zenobito are vesicular and almost aphyric with a few microphenocrysts of olivine in a groundmass of plagioclase, augite, spinel and rare biotite. High-K andesites and dacites exhibit phenocrysts of strongly zoned plagioclase, augitic clinopyroxene and minor enstatite, olivine and biotite, K-feldspar and amphibole set in a groundmass containing the same phases and glass (Gagnevin et al. 2007; Gasparon et al. 2009).

Petrology and geochemistry. Shoshonitic basalts have variable MgO, Ni, and Cr. CaO (around 7–8 wt%) and Na_2O (around 3 wt%) show some of the highest concentrations among the Tuscany mafic rocks (Fig. 2.8). There is a decrease in ferromagnesian elements and CaO, and an increase in K_2O from basalts to dacites. A group of andesites has an adakite-like composition characterised by selective enrichment in Sr-Ba-LREE and resembles the Orano dikes (Elba) and the San Vincenzo mafic enclaves. Incompatible elements patterns of Capraia mafic rocks are fractionated with strong negative anomalies of HFSE and a positive spike of Pb (Fig. 2.9b), as observed for other Tuscany mafic rocks. Sr-isotope ratios are among the lowest observed in the Tuscany Province, and increase from basalts ($^{87}Sr/^{86}Sr$ ~ 0.7081) to andesites and dacites ($^{87}Sr/^{86}Sr$ ~ 0.7087–0.7102). Sr-isotope variation has been observed among coexisting phenocrysts and within single crystals (Gagnevin et al. 2007), suggesting mixing among isotopically distinct magmas during mineral crystallisation.

Petrogenesis. Geochemical data suggest that the early high-K calcalkaline andesites and dacites evolved from mafic parents by combined fractional crystallisation and mixing (e.g. Gagnevin et al. 2007). However, the occurrence of Ba-Sr-LREE-rich andesites point to the occurrence of a distinct type of intermediate magma

(Poli and Peccerillo 2016). Interaction with lamproitic magma has been suggested to explain trace element enrichments in these rocks (Chelazzi et al. 2006). However, this contrasts with the high Sr and Ba, which show moderate to low concentrations in the lamproites, and suggest a magma origin/evolution at high pressure, outside the stability field of feldspars. The late shoshonites represent a distinct batch of magma with respect to calcalkaline activity. Their relatively high Na_2O and CaO suggest an origin in a clinopyroxene-bearing (i.e. lherzolitic) mantle. Incompatible element patterns and radiogenic isotopes require metasomatic modification of the mantle source by moderate amounts of upper crustal components.

2.6 Petrogenesis of the Tuscany Magmatic Province

According to Peccerillo (2005a, b) and Poli and Peccerillo (2016), the rock compositions of the Tuscany Magmatic Province can be considered as comprised in the space delimited by three petrologically distinct end-members (Fig. 2.13a). One end-member is silicic and displays $K_2O/Na_2O \sim 1–2$. The other two end-members are mafic, show very different K_2O/Na_2O ratios, and are classified as calcalkaline-shoshonitic basalts (CA-SHO), and high-silica lamproites (LMP).

$^{87}Sr/^{86}Sr$ versus. SiO_2 plot indicates distinct isotopic signatures for mafic CA-SHO and LMP magmas, but also reveals that the silicic end-member actually consists of three isotopically distinct groups of rock (Fig. 2.13b). Therefore, it has been stated that the petrogenetic problem of the Tuscany magmatism is that of explaining the origin of the mafic and silicic end-member magmas and of elucidating how the intermediate compositions were generated (Poli and Peccerillo 2016).

2.6.1 Origin of Silicic Magmas

A crustal anatectic origin was suggested by early authors for the Tuscany silicic magmatism (e.g. Marinelli 1975). However, several studies demonstrate that only a few silicic rocks do actually represent pure crustal anatectic melts (e.g. Poli 1992). These are labelled as Group-1 and Group-2 in Fig. 2.13b, and include some of the San Vincenzo lavas (the low-Sr, high-$^{87}Sr/^{86}Sr$ rocks), the Roccastrada rhyolites, and some leucocratic granitoid bodies occurring

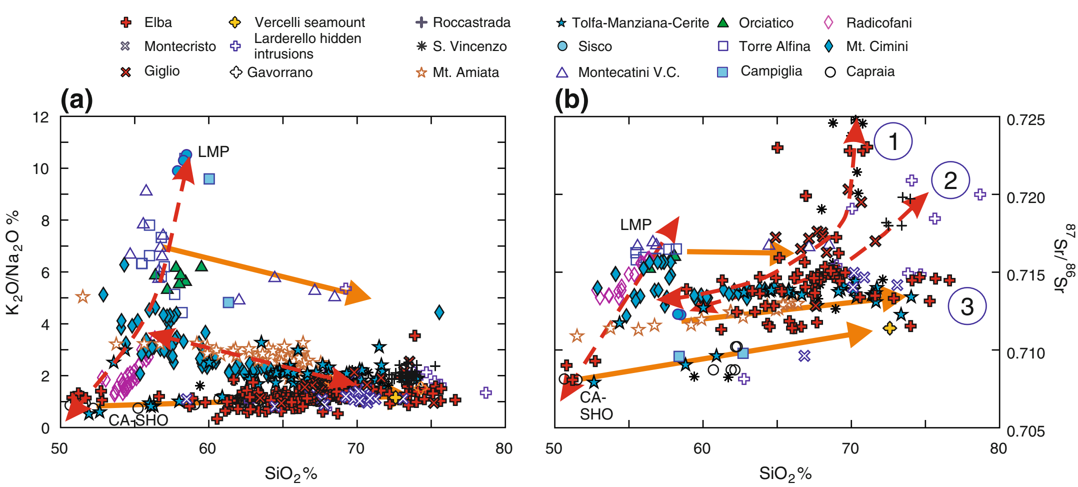

Fig. 2.13 K_2O/Na_2O and $^{87}Sr/^{86}Sr$ versus SiO_2 diagrams for the Tuscany Magmatic Province. *Dashed double-sided arrows* indicate mixing processes between various end-members; *full arrows* indicate fractional crystallisation and AFC. CA-SHO and LMP are calcalkaline-shoshonitic basalts and lamproites. Numbers in panel **b** indicate different groups of silicic rocks. For further explanation, see text

at Elba, Giglio and Larderello (e.g. Poli 1992; Westerman et al. 1993; Dini et al. 2005; Poli and Peccerillo 2016 and references therein). Note that most of these rocks contain little or no mafic enclaves, indicating scarce or no interaction with mafic melts (e.g. Pinarelli et al. 1989; Dini et al. 2005). Several studies have shown that the compositions of unmodified crustal anatectic magmas in Tuscany can be modelled by large degrees (some 40–50 %) of partial melting of garnet micaschists and gneiss, such as those found by deep drilling in Tuscany (e.g. Pinarelli et al. 1989; Poli 1992). However, Poli et al. (2002) and Poli (2004) pointed out that CaO content of many silicic granitoid rocks is exceedingly high for pelite-derived melts and advocated plagioclase-rich sources (e.g. meta-greywackes). Petrological data and geochemical modelling suggest that melting occurred in fluid-absent conditions at pressure of at least 0.4–0.6 GPa. The distinct Sr isotope ratios of Group-1 and Group-2 magmas simply indicate isotopic heterogeneities for the crustal sources, an assumption justified by the variable Sr isotope ratios of Tuscany basement rocks (see Fig. 2.6).

The majority of silicic rocks have lower Sr isotope ratios than pure crustal anatectic magmas, and exhibit clear textural and geochemical evidence (e.g. occurrence of microgranular mafic enclaves with chilled margins and crenulated edges, mafic xenocrysts, isotopic disequilibrium among coexisting phases, etc.) of interaction (i.e. mixing or mingling) between crustal anatectic and mafic magmas. The hyperbolic trends between mafic enclaves and rhyolites at San Vincenzo and Roccastrada (Fig. 2.6) have been considered as the most compelling geochemical evidence in favour of this process. Note that many granitoid and volcanic rocks fall on these trends, indicating that mixing was a widespread process operating at a regional scale. However, some rocks plot on the left-hand side of the mixing curves indicating a derivation from hybrid melts by fractional crystallisation.

The nature of mafic end-members involved in the mixing changes from one centre to the other. Poli et al. (2002) and Gagnevin et al. (2011) suggested that mafic calcalkaline melts such as those from Capraia participated in the mixing processes at Elba and Giglio. In other cases (e.g. Monte Amiata, Tolfa-Manziana-Cerite rocks), potassic to ultrapotassic mafic magmas were involved (Poli 2004).

Finally, some silicic intrusions and lavas (e.g. many aplites and leucogranites from Elba, Tolfa lavas) show relatively low $^{87}Sr/^{86}Sr \sim 0.711$–$0.715$, with respect to pure crustal anatectic melts. These may represent evolved liquids derived from intermediate hybrid parents by crystal fractionation, AFC or filter-pressing (Poli and Peccerillo 2016). These rocks plot on the left-hand side of the hyperbolic mixing trends reported in Fig. 2.6 and define the Group-3 samples in Fig. 2.13b.

In conclusion, the model summarised above supports the hypothesis that silicic rocks in Tuscany are polygenetic, and were originated by crustal melting, acid-mafic magma mixing-mingling, and fractional crystallisation starting from mafic-intermediate parents. The last process determined the formation of leucocratic rocks such as the aplitic and pegmatitic dikes and veins occurring in several intrusions.

Another theory, however, is that compositional variation of silicic rocks in Tuscany is primary, i.e. reflects variable source compositions and melting processes (e.g. Farina et al. 2012, 2014). Factors that favour formation of different magma types during crustal anatexis include composition of phases that participate in the melting reactions and the degree of entrainment within the magma of the peritectic assemblages produced during incongruent melting of the source (e.g. garnet and cordierite produced by fluid-absent melting of biotite). The isotopic variation observed in the minerals and host rocks (e.g. at Monte Capanne; Farina et al. 2014) would reflect the transitions from melting of more strongly radiogenic minerals such as muscovite and biotite, typical of metapelites, to the involvement of less radiogenic phases such as amphibole, typical of metavolcanics. Melting of different rock types could be an effect of temperature variations within the crust. According to this view, microgranular mafic enclaves and late mafic dikes associated with silicic rocks may well represent mantle-derived magmas, but they would have a minor role in determining the observed compositional variations of silicic magmas (Farina et al. 2012, 2014).

2.6.2 Origin of Mafic Magmas

The compositions of mafic rocks in Tuscany are characterised by the coexistence of both mantle and crustal signatures. The high MgO, Ni and Cr concentrations are typical of primitive mantle-derived melts. On the other hand, incompatible element abundances and ratios, high Sr- and low Nd-, Hf and Pb-isotope ratios are close or within the field of upper crustal rocks. Therefore, petrological and geochemical data provide compelling evidence for the participation of both crustal and mantle components to the origin of mafic magmas in Tuscany. The highly primitive signatures and the occurrence of ultramafic xenoliths in some rocks exclude that mantle-crust interaction occurred during magma emplacement to the surface (*magma contamination*), and clearly point to the introduction of upper crustal rocks into the mantle (*mantle contamination* or *metasomatism*). This was likely provided by subduction, but there is debate on the timing of such a process, and on the nature, origin and mechanisms of contamination. Other controversial issues include the composition of pre-metasomatic mantle rocks, the mineralogical-geochemical modifications induced by metasomatism, and the mechanisms of mantle melting (e.g. Peccerillo et al. 1987; Conticelli and Peccerillo 1992; Serri et al. 1993; Conticelli et al. 2010, 2011; Poli and Peccerillo 2016).

The high MgO and K_2O and low CaO, Na_2O, and Al_2O_3 of Tuscany lamproites suggest an origin from an ultramafic rock containing a K-rich phase, most probably phlogopite or K-richterite (e.g. Harlow and Davies 2004), and little Ca- and Al-rich minerals such as clinopyroxene and Al-spinel or garnet. Therefore, a phlogopite-harzburgite is the best candidate as source rock of lamproites, a conclusion that applies to lamproitic occurrences worldwide (e.g. Foley et al. 1987; Mitchell and Bergman 1991; Prelevic et al. 2005).

Such a hypothesis is strongly supported by experimental evidence. Investigation on simplified and natural mantle systems demonstrates that melts derived from a phlogopite-bearing peridotite at 1.0–1.5 GPa are saturated to oversaturated in silica, and become undersaturated in silica with increasing pressure (e.g. Wendlandt and Eggler 1980a,b; Foley 1992; Sato 1997; Melzer and Foley 2000; Conceição and Green 2004; Condamine and Médard 2014). Melting phase relationships demonstrate that compositions similar to Tuscany lamproites (high silica, low CaO and Na_2O), but somewhat less strongly enriched in potassium, can be generated at a pressure of 1.0 GPa and 1150–1200 °C, by about 7–13 % fluid-absent partial melting of phlogopite-harzburgite (Condamine and Médard 2014).

The occurrence of phlogopite or other K-rich phases in the mantle sources of potassic magmas requires contamination or metasomatism by K-rich material. Peccerillo et al. (1988) and Peccerillo and Martinotti (2006) noticed that incompatible element patterns of lamproites (Fig. 2.9) resemble very closely upper crustal siliceous rocks such as gneiss, crustal anatectic rhyolites, and the Global Subducted Sediments (GLOSS; Plank and Langmuir 1998). Therefore, it was suggested that introduction of siliceous upper crustal rocks into the mantle wedge was the cause of metasomatic modification of the lamproitic magma sources in Tuscany. Turbiditic sediments have been proposed as contaminants on the basis of Hf–Nd isotopic data by Prelevic et al. (2010), but other types of silicic rocks, e.g. or pelagic sediments (Gasperini et al. 2002) or material provided by erosion along the subduction channel (Vannucchi et al. 2010, 2012; Remitti et al. 2013), cannot be excluded. The close similarity of incompatible element patterns between the upper crust and Tuscany lamproites suggests that there was a mass transfer of chemical components from sediments to the mantle and hence to magmas, with little element fractionation. Notable exceptions are represented by HREE that are very fractionated in the Tuscany magma, requiring residual garnet during magma genesis. Therefore, it has been concluded that physical mixtures of sediments and harzburgites were the source of lamproitic magmas (Peccerillo and Martinotti 2006). However, the mechanisms of sediment transport and mixing are enigmatic and controversial.

Combined numerical modelling and petrological, geophysical and geochemical studies (e.g. Gerya and Yuen 2003; Gerya et al. 2006; Castro and Gerya 2008; Castro et al. 2010; Marschall and Schumacher 2012) offer an interesting scenario for interaction between mantle and bulk crust above subduction slabs. It has been suggested that a chaotic mixture of sediments, slices of oceanic crust and mantle rocks (subduction mélange) can develop at the interface between the subducting plate and the mantle wedge. Subduction mélange bodies have lower density than the surrounding mantle rocks, if sufficient amounts of sediments are involved (Behn et al. 2011). Therefore, they may rise buoyantly as diapirs or cold plumes from the surface of the slab to the hotter overlying mantle wedge. Here, diapirs undergo release of aqueous fluids and melts that migrate upward inducing metasomatism in the surrounding peridotite. Magmas can originate both in the mélange and in the metasomatic mantle around the diapirs. Tumiati et al. (2013) have shown that phlogopite is a ubiquitous phase in the mantle rocks around subduction mélange bodies and that this mineral melts preferentially to give potassic magmas.

Based on these models, it is has been suggested that mélange diapirs formed by a mixture of mantle harzburgites and subducted silicic sediments represent the source of lamproitic rocks in Tuscany (Peccerillo and Frezzotti 2015; Poli and Peccerillo 2016). Simple mass balance calculation indicates the participation of about 15 % sediment to mixing, in order to explain isotopic compositions of Tuscany lamproites (Peccerillo et al. 1988).

However, the lack of Pb positive spikes and high La/U at Sisco require a somewhat distinct type of contaminant or/and mechanism of element transfer and/or pre-metasomatic sources for this rock (Conticelli et al. 2009a,b). Speculatively, the deficiency of Pb and other LILE relative to Tuscany lamproites may reflect a minor role of transfer by fluid phases during metasomatism.

Calcalkaline and shoshonitic mafic rocks have similar incompatible element patterns but lower absolute element enrichments and less radiogenic Sr-isotope compositions than lamproites. This indicates the participation of a lower amount of crustal material. However, contents of CaO, Al_2O_3, and Na_2O increase from lamproites to calcalkaline-shoshonitic magmas, requiring the participation of other components to melting, which were scarce or absent in the source of lamproites. Therefore, it has been suggested that cpx- and spinel- or garnet-bearing rocks (i.e. spinel or garnet lherzolites rather than harzburgites) are the source of calcalkaline and shoshonitic magmas (e.g. Peccerillo and Frezzotti 2015; Poli and Peccerillo 2016). This is supported by experimental data on phlogopite-rich lherzolite whose melting (around 10–20 %) at about 1 GPa gives liquids very similar to Radicofani shoshonites (Condamine and Médard 2014). The increase from lamproitic to calcalkaline magmas of some ferromagnesian elements that are hosted by clinopyroxene, such as Sc (Fig. 2.8d), agrees with a greater involvement of this phase in the origin of calcalkaline magmas. The relatively low Cr/(Cr + Al) of chromite inclusions in olivine from shoshonitic magmas (Fig. 2.11b) provides further support to a magma origin from lherzolitic sources.

An alternative hypothesis for the formation of calcalkaline to lamproitic magmas has been proposed by Conticelli et al. (2009a, 2011, 2015a with references). According to these authors, the Tuscany mafic magmas were generated in a residual lithospheric mantle cut by veins rich in phlogopite formed by infiltration of supercritical fluids or melts from subducted sediments. Low degrees of partial melting affected prevalently the phlogopitic veins, generating lamproitic magmas. Successively, melting involved the mantle around the veins, which produced depleted melts. These mixed with early formed lamproitic magmas to give diluted calcalkaline and shoshonitic compositions.

This hypothesis, although simple and elegant, fails to explain some first-order petrological and geochemical data. First of all, if the source rocks of lamproites have a phlogopite-harzburgite composition, as generally accepted, progressive melting would dilute concentrations in early liquids not only for potassium, but also for other oxides such as Al_2O_3, CaO, and Na_2O, as clearly demonstrated by the experimental work of Condamine and Médard (2014). However, these oxides increase from lamproitic to calcalkaline magmas in Tuscany (Fig. 2.8). Another objection is that about 80–90 % of a basaltic-like melt is necessary to dilute potassium and incompatible elements contents of lamproitic liquids to the much lower levels of calcalkaline magmas. This requires extensive mantle melting, which is improbable especially for an area where volumes of mafic magmas are very low (Poli and Peccerillo 2016).

Finally, the origin of mafic rocks with intermediate compositions between calcalkaline-shoshonitic basalts and lamproites, sometimes occurring at single volcanoes, can be simply explained by mixing of extreme end-member melts. This hypothesis leads to the conclusion that distinct but closely associated harzburgitic and lherzolitic rocks occurred in the upper mantle beneath some volcanoes. These melted contemporaneously generating calcalkaline-shoshonitic and lamproitic melts that mixed during ascent to give a continuous suite of magmas with variable petrological, geochemical and isotopic characteristics (Poli and Peccerillo 2016). However, the adakite-like Sr-Ba-LREE rich intermediate compositions found at Capraia, Elba-Orano dikes and among San Vincenzo enclaves represent a distinct type of intermediate magma. This could be generated either by basalt melting in a thickened lower crust, along the subducted slab, or within the subduction mélanges, or also by high-pressure fractional crystallisation of mantle melts (e.g. Ribeiro et al. 2016).

2.7 Geodynamic Implications

The mafic rocks of the Tuscany Province show strong geochemical and isotopic differences with respect to other mantle-derived magmas in Central Italy, such as the Roman and Intra-Apennine provinces. This calls for the occurrence of distinct and possibly dyachronous metasomatic processes for these nearby magmatic districts.

It has been long suggested that mantle contamination beneath Central Italy is related to addition of different types of subducted sediments, consisting of siliceous rocks in Tuscany and carbonated pelites (marls) in the Roman and Intra-Apennine provinces (Peccerillo et al. 1988). Such a hypothesis received much support by recent geochemical ad experimental investigation (e.g. Prelevic et al. 2008, 2010; Avanzinelli et al. 2009; Conticelli et al. 2009a, b, 2010, 2011; Grassi et al. 2012). The distinct types of contamination explain the petrological and geochemical diversities of Tuscany mafic magmas with respect to other volcanoes in Central Italy.

According to Serri et al. (1993) siliceous and carbonate-rich sediments were both introduced into the sub-Apennine upper mantle by the west-dipping delaminated Adriatic continental plate from Early Miocene to Present. Such a hypothesis, however, leaves some questions unanswered. In particular, it is not clear why a single subduction process of the same slab provided two contrasting types of contaminants to the mantle sources of contiguous and partially superimposed areas. It also remains unclear why the mantle rocks contaminated by siliceous sediments beneath Tuscany melted much earlier (14.5–0.3 Ma) than the marl-contaminated mantle sources of the Roman and Intra-Apennine provinces (<0.8 Ma old).

According to Peccerillo (1999, 2002) and Peccerillo and Martinotti (2006), the variable ages of magmatism and the distinct nature of metasomatism in Tuscany and in the Roman and Intra-Apennine provinces can be better explained by assuming two mantle contamination events, occurred at different times during the evolution of the Alps-Apennine system.

A most popular hypothesis on the evolution of the Alpine-Apennine orogens submits that Cretaceous to Present convergence between Africa and Europe was first accomplished by east-directed subduction of the Alpine Tethys and European crust beneath the northern African margin (Upper Cretaceous to Eocene: Alpine stage), and successively by a new west-directed subduction process of the Neotethys-Adriatic-Ionian lithosphere (Lutetian to Present: Apennine stage) beneath the southern European margin (e.g. Doglioni et al. 1999; Carminati et al. 2010). More discussion on this topic can be found in Chap. 13.

Peccerillo (1999, 2002) and Peccerillo and Martinotti (2006) proposed that the mantle metasomatic contaminations by siliceous sediments and marls in Central Italy are diachronous and respectively occurred during the Alpine and Apennine subduction stages. The contrasting compositions of contaminants are explained by their different origin, i.e. from the subducted European and Adriatic plates, respectively. According to this hypothesis, the subduction-contamination-magma genesis history in Tuscany can be summarised as follows (Fig. 2.14):

1. Introduction of siliceous upper crustal rocks into the mantle wedge took place during the Cretaceous to Eocene south-eastward subduction of the Alpine Tethys and fragments of European continent beneath the northern African margin (Alpine stage subduction). The ultra-high pressure rocks of the Dora Maira massif represent the most compelling evidence for subduction of upper continental crust (e.g. Chopin 1984; Cadoppi 1990; Compagnoni 2003). Contamination affected the lithospheric mantle of the northern African margin probably along the entire belt going from the Betic Cordillera to Central Italy and the Western Alps (Peccerillo and Martinotti 2006). Mechanical mixing of upper crustal rocks, slices of oceanic crust

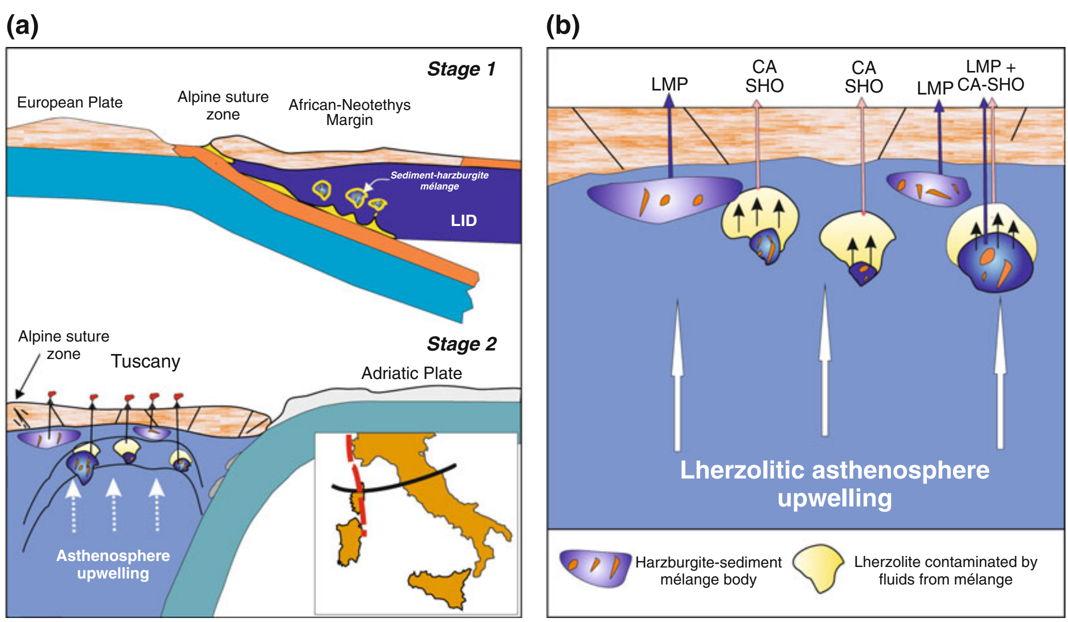

Fig. 2.14 Cartoon showing a two-stage model of mantle contamination and melting for the Tuscany Magmatic Province (modified after Poli and Peccerillo 2016). **a** *Stage 1*: Upper Cretaceous to Eocene "Alpine" subduction-collision between European and African plates brought siliceous upper crustal material into the lithospheric mantle beneath the African margin. Mélange bodies made of metasediments, slices of oceanic crust and harzburgitic mantle rocks were formed above the slab. *Stage 2*: Subduction inversion from Eocene to present generated backarc spreading, lithospheric breakup, and ascent of hot lherzolitic asthenospheric mantle. This induced dehydration and melting of Alpine mélange bodies, and metasomatism in the surrounding lherzolitic rocks. Melting of the subduction mélange bodies (*blue blobs*) gave lamproitic magmas whereas melting of metasomatised lherzolite around mélange bodies (*yellow blobs*) gave calcalkaline to shoshonitic magmas. Location of section (*black line*) and traces of the Alpine suture zone (*red dashed line*) are reported in the *Inset*. **b** Blow-up of the mantle wedge beneath Tuscany showing the origin of lamproitic (LMP) and of calcalkaline-shoshonitic (CA, SHO) magmas

and lithospheric harzburgitic mantle formed subduction mélange bodies above the slab surface. These, however, were unable to ascent much through the rigid lithospheric mantle and escaped melting, likely because of the low temperature regime along the subduction zone.

2. Starting from the Lutetian, a new west-directed subduction process developed with immersion of the Neotethys-Ionian-Adriatic lithosphere beneath the Alpine-Betic retrobelt (Apennine-Maghrebian subduction stage). Backarc extension behind the westward immerging slab prompted stretching and dismembering of the lithosphere contaminated during the Alpine subduction stage (Gueguen et al. 1997, 1998). Spreading also favoured upwelling of hot asthenosphere into the mantle wedge. Therefore, fragments of harzburgite-metapelite mélange bodies that formed during the Alpine stage were embodied into newly emplaced hot asthenospheric rocks that likely had lherzolitic composition. Mélange bodies underwent strong dehydration and melting, with fluid migration both within the mélange and from this to the surrounding newly emplaced lherzolitic mantle. Melting in the mélange body (sediments plus harzburgites) generated lamproitic magmas, whereas melting in metasomatized lherzolites around mélange bodies formed calcalkaline to shoshonitic magmas (Peccerillo and Frezzotti 2015; Poli and Peccerillo 2016). Fluid transfer phenomena may have played a minor role as a contaminant for the Sisco lamproite, a hypothesis suggested by depletion in Pb and other fluid-mobile trace elements at Sisco relative to Tuscany lamproites.
3. Miocene to present subduction of the Adriatic continental crust brought new types of sediments (i.e. marls) down into the mantle wedge, which was formed by newly emplaced lherzolitic rocks ascended from the asthenosphere during backarc spreading. Such a newly contaminated lherzolitic mantle made up the source of the Roman Province. The effects of this new contamination process were particularly important in Latium, but are also recognisable in some late centres of the Tuscany Province (e.g. Radicofani and Cimini; Peccerillo et al. 1987; Peccerillo 1999; Conticelli et al. 2013; Peccerillo and Frezzotti 2015).

A different geodynamic scenario is envisaged by Bell et al. (2013). According to these authors, a pre-Alpine contamination event affected a wide mantle sector in Central Italy and Western Alps. This successively interacted with FOZO-type mantle, producing heterogeneous sources that gave the compositionally variable magmas along the Italian peninsula. Such a hypothesis will be further discussed in Chap. 13 and Appendix 1. Here, it is only recalled that compositions as the Tuscany lamproites are not restricted to Italy but occur at several places along the Alpine-Himalayan belt and that ages and geodynamic evidence strongly supports an Alpine stage contamination for their mantle sources. Moreover, there is significant evidence that isotopic variations along the Italian do not result from simple two-end-member mixing as envisaged by Bell et al. (2004, 2013) and many others. Rather there were different mantle and crustal end-members participating in the mixing, as it will be discussed in Chap. 13 and Appendix 1.

2.8 Summary and Conclusions

The Tuscany Magmatic Province consists of an association of calcalkaline to lamproitic mafic to intermediate magmas and silicic intrusive and effusive rocks. Silicic magmas are polygenetic and have been formed by crustal melting, mixing between crustal anatectic and minor amounts of mafic melts, and fractional crystallisation or AFC starting from intermediate-mafic parents. Mafic melts originated in the mantle but resemble closely some upper crustal rocks in terms of incompatible trace element and radiogenic isotope signatures. The particular composition of these magmas reveals anomalous sources, consisting of upper mantle rocks that underwent contamination by subducted upper crustal siliceous material, such as metapelites.

Mantle contamination beneath Tuscany probably took place during the Late Cretaceous to Eocene subduction of the European plate beneath the African margin. Magmatism is much younger and occurred from Miocene to present during the opening of the northern Tyrrhenian Sea behind the west dipping subducted Adriatic plate. Tuscany magmatism becomes younger from west to the east, following the eastward backarc extension migrating in the same direction (Boccaletti et al. 1990).

The ascent of mafic magmas into the crust induced anatexis and formation of peraluminous, highly silicic magmas. These emplaced either as unmodified melts or mixed with different types of mantle-derived magmas giving hybrid products. Fractional crystallisation of hybrid magmas gave high-silica aplites and pegmatites, which are commonly found in many granitoid bodies in Tuscany.

References

Abbate E, Bortolotti V, Passerini P, Sagri M (1970) Introduction to the geology of Northern Apennines. Sedim Geol 4:521–558

Acocella V, Mulugheta G (2001) Surface deformation induced by pluton emplacement: the case of Amiata (Italy). Phys Chem Earth 26:355–362

Arai S (1994) Compositional variation of olivine–chromian spinel in Mg-rich magmas as a guide to their residual spinel peridotites. J Volcanol Geoth Res 59:279–293

Aulinas M, Gasperini D, Gimeno D, Macera P, Fernandez-Turiel JL, Cimarelli C (2011) Coexistence of calc-alkaline and ultrapotassic alkaline magmas at Mounts Cimini: evidence for transition from the Tuscan to the Roman magmatic provinces (Central Italy). Geol Acta 9:103–125

Avanzinelli R, Lustrino M, Mattei M, Melluso L, Conticelli S (2009) Potassic and ultrapotassic magmatism in the circum-Tyrrhenian region: the role of carbonated pelitic vs. pelitic sediment recycling at destructive plate margin. Lithos 113:213–227

Balestrieri ML, Pandeli E, Bigazzi G, Carosi R, Montomoli C (2011) Age and temperature constraints on metamorphism and exhumation of the syn-orogenic metamorphic complexes of Northern Apennines, Italy. Tectonophysics 509:254–271

Barberi F, Innocenti F, Mazzuoli R (1967) Contributo alla conoscenza chimico-petrografica e magmatologica delle rocce intrusive, vulcaniche e filoniane del Campigliese (Toscana). Mem Soc Geol It 6:643–681

Barberi F, Innocenti F, Ricci CA (1971) La Toscana Meridionale. Il magmatismo. Rend Soc It Min Pet 27:169–210

Barbieri M, Gasparotto G, Lucchini F, Savelli C, Vigliotti L (1986) Contributo allo studio del magmatismo del Mar Tirreno: l'intrusione granitica tardo-Miocenica del monte submarino Vercelli. Mem Soc Geol It 36:41–54

Barchi M (2010) The neogene-quaternary evolution of the Northern Apennines: crustal structure, style of deformation and seismicity. In: Beltrando M, Peccerillo A, Mattei M, Conticelli S, Doglioni C (eds) Journal virtual explorer 36, paper 11 doi:10.3809/jvirtex.2010.00220

Barchi M, Landuzzi A, Minelli G, Pialli G (2001) Outhern Northern Apennines. In: Vai GB, Martini PI (eds) Anatomy of an Orogen. The Apennines and the adjacent Mediterranean basins. Kluwer, Dordrecht, pp 215–254

Barnekow P (2000) Volcanic rocks from central Italy: an oxygen isotopic microanalytical and geochemical study. PhD thesis, University of Gottingen, 99 pp

Behn MD, Kelemen PB, Hirth G, Hacker BR, Massonne H-J (2011) Diapirs as the source of the sediment signature in arc lavas. Nat Geosci 4:641–646

Bell K, Castorina F, Lavecchia G, Rosatelli G, Stoppa F (2004) Is there a mantle plume below Italy? EOS 85:541–547

Bell K, Lavecchia G, Rosatelli G (2013) Cenozoic Italian magmatism—isotope constraints for possible plume-related activity. J South Am Earth Sci 41:22–40

Bellon, H (1981) Chronologie radiométrique (K–Ar) des manifestations magmatiques autour de la Méditerranée occidentale entre 33 Ma. et 1 Ma. In: Wezel FC (ed) Sedimentary basins of mediterranean margins, Tecnoprint Bologna, pp 341–360

Benoit MH, Torpey M, Liszewski K, Levin V, Park J (2011) P and S wave upper mantle seismic velocity structure beneath the northern Apennines: new evidence for the end of subduction. Geochem Geophys Geosyst 12:Q06004. doi:10.1029/2010GC003428

Bertagnini A, De Rita D, Landi P (1995) Mafic inclusions in the silica-rich rocks of the Tolfa-Ceriti-Manziana volcanic district (Tuscan Province, Central Italy): chemistry and mineralogy. Min Pet 54:261–276

Bianco C, Brogi A, Caggianelli A, Giorgetti G, Liotta D, Meccheri M (2015) HP-LT metamorphism in Elba Island: implications for the geodynamic evolution of the inner Northern Apennines (Italy). J Geodyn 91:13–25

Boccaletti M, Calamita F, Deiana G, Gelati R, Massari F, Moratti G, Ricci Lucchi F (1990) Migrating foredeep-thrust belt systems in the northern Apennines and southern Alps. Palaeogeogr Palaeocl 77:3–14

Boccaletti M, Gianelli G, Sani F (1997) Tectonic regime, granite emplacement and crustal structure in the inner zone of the Northern Apennines (Tuscany, Italy): a new hypothesis. Tectonophysics 270:127–143

Borelli E, Groppelli G, Aldighieri B, Battaglia A, Gamba A, Gasparon M, Malara F, Pasquaré G, Serri G, Testa B, Wijbrans J (2003) Evoluzione geologica dell'Isola di Capraia (Arcipelago Toscano) nel quadro della geodinamica del Tirreno settentrionale. In: Capozzi R (ed) Geology of the Tyrrhenian sea and Apennines, Geoacta 2:19–22
Borgia A, Mazzoldi A, Brunori CA, Allocca C, Delcroix C, Micheli L, Vercellino A, Grieco G (2014) Volcanic spreading forcing and feedback in geothermal reservoir development, Amiata Volcano, Italia. J Volcanol Geoth Res 284:16–31
Borsi S, Ferrara G, Tongiorgi E (1967) Determinazione con il metodo K/Ar delle età delle rocce magmatiche della Toscana. Boll Soc Geol It 86:403–410
Brogi A, Lazzarotto A, Liotta D, Gii Ranalli et al (2005) Crustal structures in the geothermal areas of southern Tuscany (Italy): insights from the CROP 18 deep seismic ref lection lines. J Volcanol Geoth Res 148:60–80
Brogi A, Liotta D, Meccheri M, Fabbrini L (2010) Transtensional shear zones controlling volcanic eruptions: the middle Pleistocene Mt. Amiata volcano (inner Northern Apennines, Italy). Terra Nova 22:137–146
Brunet C, Monié P, Jolivet L, Cadet JP (2000) Migration of compression and extension in the Tyrrhenian Sea, insights from $^{40}Ar/^{39}Ar$ ages on micas along a transect from Corsica to Tuscany. Tectonophysics 321: 127–155
Buttinelli M, Chiarabba C, Anselmi M, Bianchi I, De Rita D, Quattrocchi F (2014) Crustal structure of Northern Latium (central Italy) from receiver functions analysis: new evidences of a post-collisional back-arc margin evolution. Tectonophysics 621: 148–158
Cadoppi P (1990) Geologia del basamento cristallino nel settore settentrionale del massiccio Dora Maira, Alpi occidentali. PhD thesis, University of Tourin, Italy, 208 pp
Cadoux A, Pinti DL (2009) Hybrid character and pre-eruptive events of Mt. Amiata volcano (Italy) inferred from geochronological, petr-geochemical and isotopic data. J Volcanol Geoth Res 179:169–190
Cadoux A, Blichert-Toft J, Pinti DL, Albarede F (2007) A unique lower mantle source for Southern Italy volcanics. Earth Planet Sci Lett 259:227–238
Carannante S, Monachesi G, Cattaneo M, Amato A, Chiarabba C (2013) Deep structure and tectonics of the northern-central Apennines as seen by regional-scale tomography and 3-D located earthquakes. J Geophys Res 118:1–13 doi:10.1002/jgrb.50371
Carmignani L, Kligfield R (1990) Crustal extension in the northern Apennines: the transition from compression to extension in the Alpi Apuane complex. Tectonics 9:1275–1305
Carmignani L, Decandia FA, Disperati L, Fantozzi PL, Kligfield R, Lazzarotto A, Liotta D, Meccheri M (2001) Inner Northen Apennines. In: Vai GB, Martini PI (eds) Anatomy of an orogen. The Apennines and the adjacent Mediterranean basins. Kluwer, Dordrecht, pp 197–213
Carminati E, Lustrino M, Cuffaro M, Doglioni C (2010) Tectonics, magmatism and geodynamics of Italy: what we know and what we imagine. In: Beltrando M, Peccerillo A, Mattei M, Conticelli S, Doglioni C (eds) Journal virtual explorer 36, paper 9 doi:10.3809/jvirtex.2010.00226
Casagli A (2009) Studio petrografico e petrologico degli xenoliti peridotitici nelle lave lamproitiche di Torre Alfina (Lazio). MSc thesis, University of Siena, 126 pp
Castro A, Gerya TV (2008) Magmatic implications of mantle wedge plumes: experimental study. Lithos 103:103–148
Castro A, Gerya T, Garcia-Casco A, Fernandez C, Diaz Alvarado J, Moreno-Ventas I, Loew I (2010) Melting relations of MORB–sediment mélanges in underplated mantle wedge plumes. Implications for the origin of cordilleran-type batholiths. J Pet 51:1267–1295
Cellai D, Conticelli S, Menchetti S (1994) Crystal-chemistry of clinopyroxenes from potassic and ultra-potassic rocks in central Italy: implications for their genesis. Contrib Min Pet 116:301–315
Chelazzi L, Bindi L, Olmi F, Menchetti S, Peccerillo A, Conticelli S (2006) A lamproitic component in the high-K calc-alkaline and shoshonitic volcanic rocks of the Capraia Island, Tuscan Magmatic province: evidence from clinopyroxene crystal chemical data. Per Min 75:75–94
Chopin C (1984) Very-high-pressure metamorphism in western Alps: implications for subduction of continental crust. Phil Trans R Soc Lond A321:183–197
Cimarelli C, De Rita D (2006a) Relatively rapid emplacement of dome-forming magma inferred from strain analyses: the case of the acid Latian dome complexes (Central Italy). J Volcanol Geoth Res 158:106–116
Cimarelli C, De Rita D (2006b) Structural evolution of the Pleistocene Cimini trachytic volcanic complex (Central Italy). Bull Volcanol 68: 538–548 doi:10.1007/s00445-005-0028-3
Civetta L, Orsi G, Scandone P, Pece R (1978) Eastwards migration of the Tuscan anatectic magmatism due to anticlockwise rotation of the Apennines. Nature 276:604–606
Clausen C, Holm PM (1990) Origin of acid volcanics of the Tolfa district, Tuscan Province, central Italy: an elemental and Sr-isotopic study. Contrib Min Pet 105:403–411
Cocchi L, Masetti G, Muccini F, Carmisciano C (2015) Geophysical mapping of Vercelli Seamount: implications for Mioceneevolution of the Tyrrhenian back arc basin. Geosci Front 2015:1–15
Compagnoni R (2003) HP metamorphic belt of the western Alps. Episodes 26:200–204
Conceição RV, Green DH (2004) Derivation of potassic (shoshonitic) magmas by decompression melting of phlogopite + pargasite lherzolite. Lithos 72:209–229
Condamine P, Médard E (2014) Experimental melting of phlogopite-bearin mantle at 1GPa: implications for potassic magmatism. Earth Planet Sci Lett 397:80–92

Conticelli S (1998) The effect of crustal contamination on ultrapotassic magmas with lamproitic affinity: mineralogical, geochemical and isotope data from the Torre Alfina lavas and xenoliths, Central Italy. Chem Geol 149:51–81

Conticelli S, Peccerillo A (1990) Petrological significance of high-pressure ultramafic xenoliths from ultrapotassic rocks of Central Italy. Lithos 24:305–322

Conticelli S, Peccerillo A (1992) Petrology and geochemistry of potassic and ultrapotassic volcanism in Central Italy: petrogenesis and inferences on the evolution of the mantle sources. Lithos 28:221–240

Conticelli S, Manetti P, Menichetti S (1992) Mineralogy, geochemistry and Sr isotopes in orendites from South Tuscany: constraints on their genesis and evolution. Eur J Min 4:1359–1375

Conticelli S, Bortolotti V, Principi G, Laurenzi M, Vaggelli G, D'Antonio M (2001) Petrology, mineralogy and geochemistry of a mafic dyke from Monte Castello, Elba Island, Italy. Ofioliti 26:249–262

Conticelli S, D'Antonio M, Pinarelli L, Civetta L (2002) Source contamination and mantle heterogeneity in the genesis of Italian potassic and ultrapotassic volcanic rocks: Sr–Nd–Pb isotope data from Roman Province and Southern Tuscany. Min Pet 74:189–222

Conticelli S, Carlson RW, Widom E, Serri G (2007) Chemical and isotopic composition (Os, Pb, Nd and Sr) of Neogene to quaternary calc-alkalic, shoshonitic, and ultrapotassic mafic rocks from the Italian peninsula: Inferences on the nature of their sources. In: Beccaluva L, Bianchini G, Wilson M (eds) Cenozoic volcanismin the Mediterranean area. Geol Soc Am Spec Paper 418:171–202 doi:10.1130/2007.2418(09)

Conticelli S, Guarnieri L, Farinelli A, Mattei M, Avanzinelli R, Bianchini G, Boari E, Tommasini S, Tiepolo M, Prelevic D, Venturelli G (2009a) Trace elements and Sr–Nd–Pb isotopes of K-rich, shoshonitic, and calc-alkaline magmatism of the western mediterranean region: genesis of ultrapotassic to calc-alkaline magmatic associations in a post-collisional geodynamic setting. Lithos 107:68–92

Conticelli S, Marchionni S, Rosa D, Giordano G, Boari E, Avanzinelli R (2009b) Shoshonite and sub-alkaline magmas from an ultrapotassic volcano: Sr-Nd-Pb isotope data on the Roccamonfina volcanic rocks, Roman Magmatic Province, Southern Italy. Contrib Min Pet 157:41–63

Conticelli S, Laurenzi MA, Giordano G, Mattei M, Avanzinelli R, Melluso L, Tommasini S, Boari E, Cifelli F, Perini G (2010) Leucite-bearing (kamafugitic/leucititic) and -free (lamproitic) ultrapotassic rocks and associated shoshonites from Italy: constraints on petrogenesis and geodynamics. In: Beltrando M, Peccerillo A, Mattei M, Conticelli S, Doglioni C (eds) Journal virtual explorer 36, paper 20 doi:10.3809/jvirtex.2010.00251

Conticelli S, Avanzinelli R, Marchionni S, Tommasini S, Melluso L (2011) Sr-Nd-Pb isotopes from the Radicofani Volcano, Central Italy: constraints on heterogeneities in a veined mantle responsible for the shift from ultrapotassic shoshonite to basaltic andesite magmas in a post-collisional setting. Min Pet 103:123–148

Conticelli S, Avanzinelli R, Poli G, Braschi E, Giordano G (2013) Shift from lamproite-like to leucititic rocks: Sr-Nd-Pb isotope data from the Monte Cimino volcanic complex vs. the Vico stratovolcano, Central Italy. Chem Geol 353:246–266

Conticelli S, Avanzinelli R, Ammannati E, Casalini M (2015a) The role of carbon from recycled sediments in the origin of ultrapotassic igneous rocks in the Central Mediterranean. Lithos 232:174–196

Conticelli S, Boari E, Burlamacchi L et al (2015b) Geochemistry and Sr-Nd-Pb isotopes of Monte Amiata Volcano, Central Italy: evidence for magma mixing between high-K calc-alkaline and leucititic mantle-derived magmas. It J Geosci 134:266–290

Cristiani C, Mazzuoli R (2003) Monte Amiata volcanic products and their inclusions. Per Min 72:169–181

D'Orazio M, Laurenzi MA, Villa IM (1991) $^{40}Ar/^{39}Ar$ dating of a shoshonitic lava flow of the Radicofani volcanic center (Southern Tuscany). Acta Vulcanol 1:63–67

D'Orazio M, Innocenti F, Petrini R, Serri G (1994) Il vulcano di Radicofani nel quadro del magmatismo neogenico-quaternario dell'Appennino Settentrionale. Studi Geol Camerti 1:79

De Astis G, Peccerillo A, Kempton PD, La Volpe L, Wu TW (2000a) Transition from calc-alkaline to potassium-rich magmatism in subduction environments: geochemical and Sr, Nd, Pb isotopic constraints from the island of Vulcano (Aeolian arc). Contrib Min Pet 139:684–703

De Astis G, Peccerillo A, Kempton PD, La Volpe L, Wu TW (2000b) Transition from calc-alkaline to potassium-rich magmatism in subduction environments: geochemical and Sr, Nd, Pb isotopic constraints from the island of Vulcano (Aeolian arc). Contrib Min Pet 139:684–703

De Rita D, Bertagnini A, Carboni G, Ciccacci S, Di Filippo M, Faccenna C, Fredi P, Funiciello R, Landi P, Sciacca P, Vannucci N, Zarlenga F (1994) Geological-petrografical evolution of the Ceriti Mountains area (Latium, Central Italy). Mem Descr Carta Geol It 49:291–322

De Rita D, Bertagnini A, Faccenna C, Landi P, Rosa C, Zarlenga F, Di Filippo M, Carboni MG (1997) Evoluzione geopetrografica-strutturale dell'area tolfetana. Boll Soc Geol It 116:143–175

Della Vedova B, Marson I, Panza G, Suhadolc P (1991) Upper mantle properties of the Tuscan-Tyrrhenian area: a key for understanding the recent tectonic evolution of the Italian region. Tectonophysics 195:311–318

Della Vedova B, Bellani S, Pelli G, Squarci P (2001) Deep temperatures and surface heath distribution. In: Vai GB, Martini PI (eds) Anatomy of an Orogen. The Apennines and the adjacent Mediterranean basins. Kluwer, Dordrecht, pp 65–76

Della Vedova B, Vecellio C, Bellani S, Tinivella U (2006) Thermal modelling of Larderello geothermal field (Tuscany, Italy). Int J Earth Sci 97:317–332

Di Stefano R, Bianchi I, Ciaccio MG, Carrara C, Kissling E (2011) Three-dimensional Moho topography in Italy: new constraints from receiver functions and controlled source seismology. Geochem Geophys Geosyst 12:Q09006. doi:10.1029/2011GC003649
Dini A (2003) Ore deposits, industrial minerals and geothermal resources. In: Poli G, Perugini D, Rocchi S, Dini A (eds) Miocene to recent plutonism and volcanism in the Tuscan Magmatic Region (central Italy), Per Min 72:41–52
Dini A, Innocenti F, Rocchi S, Tonarini S, Westerman S (2002) The magmatic evolution of the late Miocene laccolith-pluton-dyke granitic complex of Elba Island, Italy. Geol Mag 139:257–273
Dini A, Rocchi S, Poli G (2003) Hidden granitoid from boreholes and seamounts. In: Poli G, Perugini D, Rocchi S, Dini A (eds) Miocene to recent plutonism and volcanism in the Tuscan Magmatic Region (central Italy), Per Min 72:133–138
Dini A, Gianelli G, Puxeddu M, Ruggieri G (2005) Origin and evolution of Pliocene-Pleistocene granites from the Larderello geothermal field (Tuscan Magmatic Province, Italy). Lithos 81:1–31
Dini A, Rocchi S, Westerman DS, Farina F (2009) The late Miocene intrusive complex of Elba Island: two centuries of studies from Savi to Innocenti. Acta Vulcanol 20–21:11–32
Doglioni C, Harabaglia P, Merlini S, Mongelli F, Peccerillo A, Piromallo C (1999) Orogens and slabs vs. their direction of subduction. Earth Sci Rev 45:167–208
Farina F, Dini A, Innocenti F, Rocchi S, Westerman DS (2010) Rapid incremental assembly of the Monte Capanne pluton (Elba Island, Tuscany) by downward stacking of magma sheets. Geol Soc Am Bull 122:1463–1479
Farina F, Stevens G, Dini A, Rocchi S (2012) Peritectic phase entrainment and magma mixing in the late Miocene Elba Island laccolith-pluton-dyke complex (Italy). Lithos 153:243–260
Farina F, Dini A, Rocchi S, Stevens G (2014) Extreme mineral-scale Sr isotope heterogeneity in granite by disequilibrium melting of the crust. Earth Planet Sci Lett 399:103–115
Feldstein SN, Halliday AN, Davies GR, Hall CM (1994) Isotope and chemical microsampling constraints on the history of a S-type rhyolite, San Vincenzo, Tuscany (Italy). Geochim Cosmochim Acta 58:943–958
Ferrara G, Tonarini S (1985) Radiometric geochronology in Tuscany: results and problems. Rend Soc It Min Pet 40:111–124
Ferrara G, Petrini R, Serri G, Tonarini S (1989) Petrology and isotope-geochemistry of San Vincenzo rhyolites (Tuscany, Italy). Bull Volcanol 51:379–388
Finetti IR, Boccaletti M, Bonini M, Del Ben A, Geletti R, Pipan M, Sani F (2001) Crustal section based on CROP seismic data across the North Tyrrhenian-Northen Apennines-Adriatic Sea. Tectonophysics 43:135–163
Foley SF (1992) Vein-plus-wall-rock melting mechanisms in the lithosphere and the origin of potassic alkaline magmas. Lithos 28:435–453
Foley SF, Venturelli G, Green DH, Toscani L (1987) The ultrapotassic rocks: characteristics classification, and constraints for petrogenetic models. Earth Sci Rev 24:81–134
Franceschelli M, Gianelli G, Pandeli E, Puxeddu M (2004) Variscan and Alpine metamorphic events in the Northern Apennines (Italy): a review. Per Mineral 73:43–56
Franceschini F, Innocenti F, Marsi A, Tamponi M, Serri G (2000) Petrography and chemistry of the buried Pliocene Castel di Pietra pluton (Southern Tuscany, Italy). Neues Jahrb Geol P M 215:17–46
Frondini F, Caliro S, Cardellini C, Chiodini G, Morgantini N, Parello F (2008) Carbon dioxide degassing from Tuscany and Northern Latium. Global Planet Change 61:89–102
Gagnevin D, Daly JS, Poli G (2004) Petrographic, geochemical and isotopic constraints on magma dynamics and mixing in the Miocene Monte Capanne monzogranite (Elba Island, Italy). Lithos 78:157–195
Gagnevin D, Daly JS, Poli G, Morgan D (2005) Microchemical and Sr isotopic investigation of zoned K-feldspar megacrysts: insights into the petrogenesis of a granitic system and disequilibrium crystal growth. J Petrol 46:1689–1724
Gagnevin D, Waight TE, Daly JS, Poli G, Conticelli S (2007) Insights into magmatic evolution and recharge history in Capraia Volcano (Italy) from chemical and isotopic zoning in plagioclase phenocrysts. J Volcanol Geoth Res 168:28–54
Gagnevin D, Daly JS, Kronz A (2010) Zircon texture and chemical composition as a guide to magmatic processes and mixing in a granitic environment and coeval volcanic system. Contrib Min Pet 159:579–596
Gagnevin D, Daly JS, Horstwood MSA, Whitehouse MJ (2011) In-situ zircon U-Pb, oxygen and hafnium isotopic evidence for magma mixing and mantle metasomatism in the Tuscan Magmatic Province, Italy. Earth Planet Sci Lett 305:45–56
Gale A, Dalton CA, Langmuir CH, Su Y, Schilling J-G (2013) The mean composition of ocean ridge basalts. Gechem Geophys Geosyst 14 doi:10.1029/2012GC004334
Gasparon M, Rosenbaum G, Wijbrans J, Manetti P (2009) The transition from subduction arc to slab tearing: evidence from Capraia Island, northern Tyrrhenian Sea. J Geodyn 47:30–38
Gasperini D, Blichert Toft J, Bosch D, Del Moro A, Macera P, Albaréde F (2002) Upwelling of deep mantle material through a plate window: evidence from the geochemistry of Italian basaltic volcanics. J Geophys Res 107(B12):2367. doi:10.1029/2001JB000418
Gerya T, Yuen DA (2003) Rayleigh-Taylor instabilities from hydration and melting propel 'cold plumes' at subduction zones. Earth Planet Sci Lett 212:47–62

Gerya TV, Connolly JAD, Yuen DA, Gorczyk W, Capel AM (2006) Seismic implications of mantle wedge plumes. Phys Earth Planet In 156:59–74

Giacomuzzi G, Civalleri M, De Gori P, Chiarabba C (2012) A 3D Vs model of the upper mantle beneath Italy: Insight on the geodynamics of central Mediterranean. Earth Planet Sci Lett 335-336:105–120

Gianelli G, Laurenzi M (2001) Age and cooling rate of the geothermal system of Larderello. Trans Geoth Resour Counc 25:731–735

Gianelli G, Manzella A, Puxeddu M (1997) Crustal models of the geothermal areas of southern Tuscany. Tectonophysics 281:221–239

Gill R (2010) Igneous rocks and processes. A practical guide. Wiley-Blackwell, Chichester, p 428

Giraud A, Dupuy C, Dostal J (1986) Behaviour of trace elements during magmatic processes in the crust: application to silicic volcanic rocks of Tuscany. Chem Geol 57:269–288

Grassi D, Schmidt MW, Gunther D (2012) Element partitioning during carbonated pelite melting at 8, 13 and 22 GPa and the sediment signature in the EM mantle components. Earth Planet Sci Lett 327–328:84–96

Gueguen E, Doglioni C, Fernandez M (1997) Lithospheric boudinage in the Western Mediterranean back-arc basin. Terra Nova 9:184–187

Gueguen E, Doglioni C, Fernandez M (1998) On the post-25 Ma geodynamic evolution of the western Mediterranean. Tectonophysics 298:259–269

Harlow GE, Davies R (2004) Status report on stability of K-rich phases in the upper mantle. Lithos 77:647–653

Hawkesworth CJ, Vollmer R (1979) Crustal contamination vs. enriched mantle: $^{143}Nd/^{144}Nd$ and $^{87}Sr/^{86}Sr$ evidence from the Italian volcanics. Contrib Min Pet 69:151–165

Innocenti F, Westerman DS, Rocchi S, Tonarini S (1997) The Montecristo monzogranite (Northern Tyrrhenian Sea, Italy): a collisional pluton in an extensional setting. Geol J 32:131–151

Irvine TN, Baragar WRA (1971) A guide to chemical classification of common volcanic rocks. Can J Earth Sci 8:523–548

LaBerge RD, Giordano G, Cas RAF, Ailleres L (2006) Syn-depositional substrate deformation produced by the shear force of a pyroclastic density current: an example from the Pleistocene ignimbrite at Monte Cimino, northern Lazio, Italy. J Volcanol Geoth Res 148:307–320

Lardini D, Nappi G (1987) I cicli eruttivi del complesso vulcanico Cimino. Rend Soc It Min Pet 42:141–153

Lattanzi P, Benvenuti M, Costagliola P, Maineri C, Mascaro I, Tanelli G, Dini A, Ruggieri G (2001) Magmatic versus hydrotermal processes in the formation of raw ceramic material deposits in southern Tuscany. In: Proceeding 10th international symposium water-rock interaction, Villasimius (Italy), 10–15 June 2001, pp 725–728

Laurenzi MA, Balestrieri ML, Bigazzi G, Neto JCH, Iunes PJ, Norelli P, Oddone M, Osorio Araya AM, Viramonte JG (2007) New constraints on ages of glasses proposed as reference materials for fission-track dating. Geostand Geoanal Res 31:105–124

Laurenzi MA, Braschi E, Casalini M, Conticelli S (2015) New $^{40}Ar/^{39}Ar$ dating and revision of the geochronology of the Monte Amiata Volcano, Central Italy. It J Geosci 134:255–265

Le Maitre RW (ed) (2002) A classification of igneous rocks and glossary of terms. Cambridge University Press, Cambridge 252 pp

Marani MP, Gamberi F (2004) Distribution and nature of submarine volcanic landforms in the Tyrrhenian Sea: the arc versus the back-arc. Mem Descr Carta Geol It 44:109–126

Marinelli G (1975) Magma evolution in Italy. In: Squyres CH (ed) Geology of Italy. Petrol Expl Soc Libya, Tripoli, pp 165–219

Marinosci I (1993) Studio petrografico comparativo tra la minette del filone strato di Sisco (Corsica Settentrionale) e le selagiti del volterrano toscano. Geol Romana 29:237–247

Marroni M, Moratti G, Costantini A et al (2015) Geology of the Monte Amiata region, Southern Tuscany, Central Italy. It J Geosci 134:200–218

Marschall HR, Schumacher JC (2012) Arc magmas sourced from mélange diapirs in subduction zones. Nat Geosci 5:862–867

Masuda H, O'Neil R (1994) Oxygen-isotope heterogeneity of phenocrysts in rhyolite from San Vincenzo, Italy, by laser microprobe analysis. Geochem J 28:377–385

Mazzarini F, Corti G, Musumeci G, Innocenti F (2004) Tectonic control on laccolith emplacement in the northern Apennines fold-thrust belt: the Gavorrano intrusion (southern Tuscany, Italy). In: Breitkreuz C, Petford N (eds) Physical geology of high-level magmatic systems, Geol Soc London Spec Publ 234:151–161

Mazzuoli R (1967) Le vulcaniti di Roccastrada (Grosseto). Atti Soc Tosc Sci Nat A84:315–373

Mazzuoli R, Pratesi M (1963) Rilevamento e studio chimico-petrografico delle rocce vulcaniche del Monte Amiata. Atti Soc Tosc Sci Nat A70:355–429

Mele G, Sandvol E (2003) Deep crustal roots beneath the northern Apennines inferred from teleseismic receiver functions. Earth Planet Sci Lett 211:69–78

Mele G, Sandvol E, Cavinato GP (2006) Evidence of crustal thickening beneath the central Apennines (Italy) from teleseismic receiver functions. Earth Planet Sci Lett 249:425–435

Melzer S, Foley SF (2000) Phase relations and fractionation sequences in potassic magma series modelled in the system $CaMgSi_2O_6$-$KAlSiO_4$-Mg_2SiO_4-F at 1 bar to 18 kbar. Contrib Min Pet 138:186–197

Minissale A (1991) The Larderello geothermal field: a review. Earth Sci Rev 31:133–151

Minissale A, Magro G, Martinelli G, Vaselli O, Tassi GF (2000) Fluid geochemical transect in the Northern Apennines (central-northern Italy): fluid genesis and migration and tectonic implications. Tectonophysics 319:199–222

Mitchell RH, Bergman SC (1991) Petrology of lamproites. Plenum, New York 447 pp
Musumeci G, Mazzarini F, Corti G, Barsella M, Montanari D (2005) Magma emplacement in a thrust ramp anticline: the Gavorrano granite (northern Apennines, Italy). Tectonics 24, TC6009 doi:10.1029/2005TC001801
Nikogossian IK, van Bergen MJ (2010) Heterogeneous mantle sources of potassium-rich magmas in central-southern Italy: melt inclusion evidence from Roccamonfina and Ernici (Mid Latina Valley). J Volcanol Geoth Res 197:279–302
Pandeli E, Santo AP, Morelli M, Orti L (2006) Petrological and geological data of porphyritic dikes from the Capo Arco area (Eastern Elba Island, northern Tyrrhenian Sea). Per Min 75:241–154
Pandeli E, Bartolini C, Dini A, Antolini E (2010) New data on the paleogeography of Southern Tuscany (Italy) since Late Miocene time. Int J Earth Sci 99:1357–1381
Pandeli E, Santo AP, Candido MR, Petrone CM, Giusti R (2014) The calc-alkaline Monte Capo Stella dykes in the ophiolitic unit of the Elba Island (Italy): Geological setting and compositional characterization. Ofioliti 39:79–93
Panza GF, Mueller S (1979) The plate boundary between Eurasia and Africa in the Alpine area. Mem Soc Geol It 33:43–50
Pauselli C, Barchi MR, Federico C, Magnani MB, Minelli G (2006) The crustal structure of the northern Apennines (central Italy): an insight by the CROP03 seismic line. Am J Sci 306:428–450
Peccerillo A (1999) Multiple mantle metasomatism in central-southern Italy: geochemical effects, timing and geodynamic implications. Geology 27:315–318
Peccerillo A (2002) Plio-quaternary magmatism in central-southern Italy: a new classification scheme for volcanic provinces and its geodynamic implications. In: Barchi RM, Cirilli S, Minelli G (eds) Geological and geodynamic evolution of the Apennines. Boll Soc Geol It (Spec Vol 1):113–127
Peccerillo A (2005a) Plio-Quaternary volcanism in Italy. Petrology, geohemistry, geodinamics. Springer, Berlin, p 365
Peccerillo A (2005b) On the nature of carbonate-rich volcanic rocks in Central Italy. A reply to comments by Woolley et al. Per Min 74:195–204
Peccerillo A, Frezzotti ML (2015) Magmatism, mantle evolution and geodynamics at the converging plate margins of Italy. J Geol Soc Lond 172:407–427
Peccerillo A, Martinotti G (2006) The Western Mediterranean lamproitic magmatism: origin and geodynamic significance. Terra Nova 18:109–117
Peccerillo A, Taylor SR (1976) Geochemistry of Eocene calc-alkaline volcanic rocks of the Kastamonu area, northern Turkey. Contrib Min Pet 58:63–81
Peccerillo A, Conticelli S, Manetti P (1987) Petrological characteristics and the genesis of recent magmatism of Southern Tuscany and Northern Latium. Per Min 56:157–172
Peccerillo A, Poli G, Serri G (1988) Petrogenesis of orenditic and kamafugitic rocks from Central Italy. Can Min 26:45–65
Peccerillo A, De Astis G, Faraone D, Forni F, Frezzotti ML (2013) Compositional variations of magmas in the Aeolian arc: implications for petrogenesis and geodynamics. In: Lucchi F, Peccerillo A, Keller J, Tranne CA, Rossi PL (eds) The Aeolian islands volcanoes. Geol Soc London Memoirs 37:491–510
Pera E, Mainprice D, Burlini L (2003) Anisotropic seismic properties of the upper mantle beneath the Torre Alfina area (Northern Apennines, Central Italy). Tectonophysics 370:11–30
Pinarelli L (1991) Geochemical and isotopic (Sr, Pb) evidence of crust-mantle interaction in silicicic melts. The Tolfa-Cerveteri-Manziana volcanic complex (Central Italy): a case history. Chem Geol 92:177–195
Pinarelli L, Poli G, Santo A (1989) Geochemical characterization of recent volcanism from the Tuscan Magmatic Province (Central Italy): the Roccastrada and San Vincenzo centers. Per Min 58:67–96
Piromallo C, Morelli A (2003) P wave tomography of the mantle under the Alpine-Mediterranean area. J Geophys Res 108(B2):2065. doi:10.1029/2002JB001757
Plank T, Langmuir CH (1998) The chemical composition of subducting sediment and its consequences for the crust and mantle. Chem Geol 145:325–394
Poli G (1985) Phase composition in volcanic rocks from Soth Tuscany magmatic area (Central Italy): inferences on conditions of magma crystallization. Neues Jb Miner Abh 151:141–161
Poli G (1992) Geochemistry of Tuscan Archipelago granitoids, Central Italy: the role of hybridization processes in their genesis. J Geol 100:41–56
Poli G (2004) Genesis and evolution of Miocene-quaternary intermediate-acid rocks from the Tuscan Magmatic Province. Per Min 73:187–214
Poli G, Peccerillo A (2016) The upper miocene magmatism of the Elba Island: compositional characteristics, petrogenesis and implications for the origin of the Tuscany Magmatic Province. Min Pet 110:421–445
Poli G, Perugini D (2003a) San Vincenzo volcanites. In: Poli G, Perugini D, Rocchi S, Dini A (eds) Miocene to recent plutonism and volcanism in the Tuscan Magmatic Region (central Italy), Per Min 72:141–155
Poli G, Perugini D (2003b) Roccastrada volcanites. In: Poli G, Perugini D, Rocchi S, Dini A (eds) Miocene to recent plutonism and volcanism in the Tuscan magmatic region (central Italy), Per Min 72:157–168
Poli G, Perugini D (2003c) The Island of Capraia. In: Poli G, Perugini D, Rocchi S, Dini A (eds) Miocene to recent plutonism and volcanism in the Tuscan magmatic region (central Italy), Per Min 72:195–201
Poli G, Frey FA, Ferrara G (1984) Geochemical characteristics of the south Tuscany (Italy) volcanic

province, constraints on lava petrogenesis. Chem Geol 43:203–221
Poli G, Manetti P, Tommasini S (1989) A petrological review on Miocene-Pliocene intrusive rocks from Southern Tuscany and Tyrrhenian Sea (Italy). Per Min 58:109–126
Poli G, Peccerillo A, Donati C (2002) The Plio-Quaternary acid magmatism of Southern Tuscany. In: Barchi RM, Cirilli S, Minelli G (eds) Geological and geodynamic evolution of the Apennines. Boll Soc Geol It Spec 1:143–151
Poli G, Perugini D, Rocchi S, Dini A (eds) (2003) Miocene to Recent plutonism and volcanism in the Tuscan Magmatic Province. Per Mineral 72:244 pp
Prelevic D, Foley SF, Cvetkovic V, Romer RL, Downes H (2005) Tertiary ultrapotassic volcanism in Serbia: constraints on petrogenesis and mantle source characteristics. J Pet 46:1443–1487
Prelevic D, Foley SF, Romer R, Conticelli S (2008) Mediterranean tertiary lamproites derived from multiple source components in postcollisional geodynamics. Geochim Cosmochim Acta 72:2125–2156
Prelevic D, Stracke A, Foley SF, Romer RL, Conticelli S (2010) Hf isotope compositions of Mediterranean lamproites: mixing of melts from asthenosphere and crustally contaminated mantle lithosphere. Lithos 119:297–312
Principi G, Treves B (1984) Il sistema corso-appenninico come prisma d'accrezione: Riflessi sul problema generale del limite Alpi-Appennini. Mem Soc Geol It 28:549–576
Prosperini N (1993) Petrologia e geochimica delle rocce dell'isola di Capraia (Arcipelago Toscano, Italia): un vulcano calcalcalino di origine complessa. BSc thesis, University of Perugia, 149 pp
Puxeddu M (1971) Studio chimico-petrografico delle vulcaniti del M. Cimino (Viterbo). Atti Soc Tosc Sci Nat A78:329–394
Remitti F, Balestrieri ML, Vannucchi P, Bettelli G (2013) Early exhumation of underthrust units near the toe of an ancient erosive subduction zone: A case study from the Northern Apennines of Italy. Geol Soc Am Bull 125:1820–1832
Ribeiro JM, Maury RC, Grégpire M (2016) Are adakites slab melts or high-pressure fractionatedmantle melts? J Petrol 57, doi: 10.1093/petrology/egw023 (in press)
Ridolfi F, Renzulli A, Acosta-Vigil A (2014) On the stability of magmatic cordierite and new thermobarometric equations for cordierite-saturated liquids. Contrib Min Pet 167:996. doi:10.1007/s00410-014-0996-4
Rocchi S, Westerman DS, Dini A, Innocenti F, Tonarini S (2002) Two-stage growth of laccoliths at Elba Island, Italy. Geology 30:983–986
Rocchi S, Dini A, Innocenti F, Tonarini S Westerman DS, (2003a) The Elba Island: intrusive magmatism. In: Poli G, Perugini D, Rocchi S, Dini A (eds) Miocene to recent plutonism and volcanism in the tuscan magmatic region (central Italy), Per Mineral 72:73–104
Rocchi S, Westerman DS, Innocenti F (2003b) Montecristo island: intrusive magmatism. In: Poli G, Perugini D, Rocchi S, Dini A (eds) Miocene to recent plutonism and volcanism in the Tuscan magmatic region (central Italy), Per Min 72:105–118
Rocchi S, Dini A, Mazzarini F, Poli G (2003c) Campiglia Marittima and Gavorrano intrusive magmatism. In: Poli G, Perugini D, Rocchi S, Dini A (eds) Miocene to Recent plutonism and volcanism in the Tuscan Magmatic region (central Italy), Per Min 72:127–132
Rocchi S, Westerman DS, Dini A, Farina F (2010) Intrusive sheets and sheeted intrusions at Elba Island, Italy. Geosphere 6:225–236
Sato K (1997) Melting experiments on a synthetic olivine lamproite compositionup to 8 GPa: implication to its petrogenesis. J Gephys Res 102:14751–14764
Savelli C (2000) Subduction-related episodes of K-alkaline magmatism (15–0.1 Ma) and geodynamic implications in the north Tyrrhenian, central Italy region: a review. J Geodyn 30:575–591
Serri G, Innocenti F, Manetti P (1993) Geochemical and petrological evidence of the subduction of delaminated Adriatic continental lithosphere in the genesis of the Neogene-quaternary magmatism of central Italy. Tectonophysics 223:117–147
Streckeisen AL, Le Maitre RW (1979) Chemical approximation to modal QAPF classification of the igneous rocks. Neues Neues Jb Min 136:169–206
Sun SS, McDonough WF (1989) Chemical and isotopic systematics of oceanic basalts: implications for mantle composition and processes. In: Saunders AD, Norry MJ (eds) Magmatism in ocean basins. Geol Soc London Spec Publ 42:313–345
Tanelli G, Lattanzi P (1986) Metallogeny and mineral exploration in Tuscany: state of the art. Mem Soc Geol It 31:299–304
Tanelli G, Poggi L (2012) La Collezione Elbana. In: Pratesi G (ed) The museum of natural history of the University of Florence, the mineralogical and lithological collections. Florence Univ Press 4:67–81
Tarquini S, Vinci S, Favalli M, Doumaz F, Fornaciai A, Nannipieri L (2012) Release of a 10-m-resolution DEM for the Italian territory: comparison with global-coverage DEMs and anaglyph-mode exploration via the web. Comput Geosci 38:168–170
Tumiati S, Fumagalli P, Tiraboschi C, Poli S (2013) An experimental study on COH-bearing Peridotite up to 3.2 GPa and implications for crust-mantle recycling. J Pet 54:453–479
Turi B, Taylor HP (1976) Oxygen isotope studies of potassic volcanic rocks of the Roman Province, central Italy. Contrib Min Pet 55:1–31
van Bergen MJ (1985) Common trace element characteristics of crustal- and mantle-derived K-rich magmas from Monte Amiata (central Italy). Chem Geol 48:125–135
van Bergen MJ, Barton M (1984) Complex interaction of aluminous metasedimentary xenoliths and siliceous magma: an example from Mt. Amiata (Central Italy). Contrib Min Pet 86:374–385
van Bergen MJ, Ghezzo C, Ricci CA (1983) Minette inclusions in the rhyodacitic lavas of Mt. Amiata (central Italy): mineralogical and chemical evidence of

mixing between Tuscan- and Roman-type magmas. J Volcanol Geoth Res 19:1–35
Vannucchi P, Remitti F, Bettelli G, Boschi C, Dallai L (2010) Fluid history related to the early Eocene-middle Miocene convergent system of the Northern Apennines (Italy): Constraints from structural and isotopic studies. J Geophys Res 115, B05405 doi:10.1029/2009JB006590
Vannucchi P, Sage F, Morgan JP, Remitti F, Collot JY (2012) Toward a dynamic concept of the subduction channel at erosive convergent margins with implications for interplate material transfer. Geochem Geophys Geosyst 13:Q02003. doi:10.1029/2011GC003846
Villa IM, Giuliani O, De Grandis G, Cioni R (1989) Datazioni K/Ar dei vulcani di Tolfa e Manziana. Boll Gruppo Naz Vulcanol 2:1025–1026
Villa IM, Ruggieri G, Puxeddu M (2001) Geochronology of magmatic and hydrothermal micas from Larderello geothermal field. In: Cidu R (ed) Proceedings 10th international symposium water-rock interaction, Balkema 1, pp 1589–1592
Vollmer R (1976) Rb-Sr and U-Th-Pb systematics of alkaline rocks: the alkaline rocks from Italy. Geochim Cosmochim Acta 40:283–295
Vollmer R (1977) Isotopic evidence for genetic relations between acid and alkaline rocks in Italy. Contrib Min Pet 60:109–118
Wagner C, Velde D (1986) The mineralogy of K-richterite-bearing lamproites. Am Min 71:17–37
Wendlandt RF, Eggler DH (1980a) The origins of potassic magmas: 1. Melting relations in the systems $KAlSiO_4$ -Mg_2SiO_2 and $KAlSiO_4$ -MgO -SiO_2 -CO_2 to 30 kilobars. Am J Sci 280:385–420
Wendlandt RF, Eggler DH (1980b) The origins of potassic magmas: 2. Stability of phlogopite in natural spinel lherzolite an in the $KAlSiO_4$-MgO-SiO_2-H_2O-CO_2 at high pressures and high temperatures. Am J Sci 280:421–458
Westerman DS, Innocenti F, Tonarini S, Ferrara G (1993) The Pliocene intrusion of the Island of Giglio. Mem Soc Geol It 49:345–363
Westerman DS, Innocenti F, Rocchi S (2003) Giglio island: intrusive magmatism. In: Poli G, Perugini D, Rocchi S, Dini A (eds) Miocene to recent plutonism and volcanism in the Tuscan Magmatic Region (central Italy), Per Min 72:119–126
Westerman DS, Dini A, Innocenti F, Rocchi S (2004) Rise and fall of a nested Christmas-tree laccolith complex, Elba Island, Italy. In: Breitkruez C, Petford N (eds) Physical geology of high-level magmatic systems. Geol Soc Lond Spec Publ 234:195–213
Zitellini N, Trincardi F, Marani M, Fabbri A (1986) Neogene tectonics of the northern Tyrrhenian Sea. Giorn Geol 48:25–40

Springer

http://www.springer.com/978-3-319-42489-7

Cenozoic Volcanism in the Tyrrhenian Sea Region
Peccerillo, A.
2017, XX, 399 p. 170 illus., 169 illus. in color.,
Hardcover
ISBN: 978-3-319-42489-7